HAL open science

Intra- and inter-annual variability of North Brazil current rings using angular momentum Eddy detection and tracking algorithm: observations from 1993 to 2016

L.C. Aroucha, Dóris Veleda, F. S. Lopes, Pedro Tyaquiçã, Nathalie Lefèvre, Moacyr Araujo

To cite this version:

L.C. Aroucha, Dóris Veleda, F. S. Lopes, Pedro Tyaquiçã, Nathalie Lefèvre, et al.. Intra- and inter-annual variability of North Brazil current rings using angular momentum Eddy detection and tracking algorithm: observations from 1993 to 2016. Journal of Geophysical Research. Oceans, 2020, 125 (12), pp.e2019JC015921. 10.1029/2019JC015921 . hal-03145630

HAL Id: hal-03145630

https://hal.science/hal-03145630

Submitted on 23 Jun 2022

HAL is a multi-disciplinary open access archive for the deposit and dissemination of scientific research documents, whether they are published or not. The documents may come from teaching and research institutions in France or abroad, or from public or private research centers.

L'archive ouverte pluridisciplinaire **HAL**, est destinée au dépôt et à la diffusion de documents scientifiques de niveau recherche, publiés ou non, émanant des établissements d'enseignement et de recherche français ou étrangers, des laboratoires publics ou privés.

Check for updates

JGR Oceans

RESEARCH ARTICLE

10.1029/2019JC015921

Key Points:

- North Brazil Current (NBC) rings in boreal winter are larger, more energetic, faster rotating, and short living, in contrast with boreal summer and early fall
- Downwelling associated with NBC anticyclonic rings deepens thermocline and modify the vertical salinity profile
- NBC ring merging significantly increase NBC rings V_{max} and kinetic energy

Supporting Information:

- Table S1
- Table S2
- Table S3
- Table S4
- Figure S1
- Figure S2
- Figure S3
- Figure S4

Correspondence to:

L. C. Aroucha,
leo.aroucha@ufpe.br

Citation:

Aroucha, L. C., Veleda, D., Lopes, F. S., Tyaquiçã, P., Lefèvre, N., & Araujo, M.. (2020). Intra- and inter-annual variability of North Brazil Current rings using angular momentum eddy detection and tracking algorithm: observations from 1993 to 2016. *Journal of Geophysical Research: Oceans*, *125*, e2019JC015921. https://doi.org/10.1029/2019JC015921

Received 26 NOV 2019
Accepted 24 OCT 2020

© 2020. American Geophysical Union. All Rights Reserved.

Intra- and Inter-Annual Variability of North Brazil Current Rings Using Angular Momentum Eddy Detection and Tracking Algorithm: Observations From 1993 to 2016

L. C. Aroucha[1,2,3], D. Veleda[1,2], F. S. Lopes[1,2], P. Tyaquiçã[4], N. Lefèvre[4], and M. Araujo[1,5]

[1]Laboratory of Physical, Coastal and Estuarine Oceanography – LOFEC, Federal University of Pernambuco – UFPE, Recife, Brazil, [2]Renewable Energy Center – CER, Federal University of Pernambuco – UFPE, Recife, Brazil, [3]Now at Department of Oceanography - UFPE, Cidade Universitária, Recife, Brazil, [4]LOCEAN, IRD, Sorbonne Université Paris, Paris, France, [5]Center for Risk Analysis and Environmental Modeling – CEERMA, Federal University of Pernambuco – UFPE, Recife, Brazil

Abstract In order to investigate intra- and inter-annual variability of North Brazil Current (NBC) rings, angular momentum eddy detection and tracking algorithm (AMEDA) was used for identification of their occurrence, trajectories, and parameters. Based on 24 years (1993–2016) of geopotential height and geostrophic current fields reanalysis data from ARMOR 3D (¼°), we identified an average rate of five NBC rings shed by year. The rings present an average lifetime of 15.3 (±5.4) weeks, average speed-based radius (R_{max}) of 139.8 (±23.6) km, and mean sea surface height anomaly (SSHa) of 9.4 (±4.0) cm. The mean observed maximum azimuthal velocity (V_{max}) was 0.27 (±0.08) m/s, while the averaged Rossby number (Ro) value was 0.08 (±0.04) and averaged kinetic energy (KE) was of 255.3 (±154.8) cm^2/s^2. NBC rings have larger dimensions, rotate faster, live less, and transfer more energy in boreal winter months. In contrast, those shed during boreal summer and early fall last longer, have smaller diameters and carry less energy. Besides, the analysis of ring merging pointed that the interaction between NBC rings generated a significantly increase in ring energy (52%), and velocity (22%). Finally, we observed the vertical anomalies temperature and salinity profiles, which indicated a thermocline deepening and sinking of coastal and tropical waters due to NBC rings downwelling. This study emphasizes the robustness and efficiency of AMEDA for studying rings in the ocean and further theorizes possible impacts of NBC ring on ocean physical and biogeochemical features in the Western Tropical North Atlantic.

Plain Language Summary Oceanic rings are dynamical structures formed by strong current circulation, that are present in the sea like hurricanes are in the atmosphere. They can change seawater characteristics by changing the direction and velocity of ocean currents, and by carrying a parcel of water and its features (such as temperature, heat content, salinity, and nutrients) from one region to another in the ocean. Using 24 years of data, this study analyses the occurrence and characteristics of rings that originated from the North Brazil Current (NBC), in the Tropical Atlantic region. We examine how ring characteristics changed from year to year and from season to season. We use a computational algorithm that identifies and provides information about a ring based on the current direction and other physical parameters. We find that rings are larger, rotate faster, live less, and carry more energy in boreal winter months, while during boreal summer and early fall, they last longer, have smaller diameters, and carry less energy. Plus, the water flux downward associated with NBC eddies centers generates an increased in mixed layer and deepens the thermocline. Finally, we show that the when rings merge, they increase their energy and velocity.

1. Introduction

The North Brazil Current (NBC) is an intense western boundary current, which is the dominant feature of the surface circulation in the Western Tropical North Atlantic (WTNA). It flows predominantly northwestward along Brazilian northern coast and, around 6°N–8°N and 45°W, the current separates from the coast and retroflects to the east, feeding the North Equatorial Countercurrent (NECC; Garzoli et al., 2003; Johns

et al., 1990). This retroflection, which is related to the seasonal migration of the Intertropical Convergence Zone (ITCZ) (Fonseca et al., 2004), can occasionally shed large anticyclonic rings, that are associated with positive anomalies of sea surface height (SSH) in their centers, traveling northwestward until colliding with the Lesser Antilles (Didden & Schott, 1993; Fratantoni & Richardson, 2006; Jochumsen et al., 2010; Johns et al., 2003). The NBC retroflection is most developed between June and February and is nearly absent from March to May (Johns et al., 1998). However, other mechanisms, rather than the meandering current, were proposed to explain NBC rings generation. Ma (1996) and Jochum and Malanotte-Rizzoli (2003) showed that equatorial Rossby waves that propagate westward and reflect at the Brazilian coast could generate these eddies. Moreover, they intensify when traveling northwestward due to the conservation of the potential vorticity (Jochum & Malanotte-Rizzoli, 2003). The south American coastline inclination between 5°N and 8°N was shown to be important for ring generation (Zharkov & Nof, 2010). NBC rings are crucial in the interhemispheric transport of mass and heat in the Atlantic, being an essential part of the meridional overturning circulation (MOC) (Fratantoni et al., 2000; Johns et al., 2003). Furthermore, they contribute to the dispersion of fresh nutrient-rich waters from the Amazon River toward the Caribbean (Johns et al., 1990), also affecting local circulation, that influences planktonic fish larvae recruitment and growth (Cowen et al., 2003). Given the importance of those rings, their study and record of their parameters are a key to the comprehension of physical and biogeochemical processes in the WTNA.

The first study that described the presence of the NBC rings was done by Legeckis and Gordon (1982). They used satellite sea surface temperature (SST) data to identify elliptical warm-core rings that move northwestward with velocities from 4 to 35 km/day (Legeckis & Gordon, 1982). In the following years, a number of studies contributed to the understanding of NBC rings dimensions and dynamics (Didden & Schott, 1993; Fratantoni et al., 1995; Johns et al., 1990; Pauluhn & Chao, 1999; Richardson et al., 1994), especially after the 1998–2001 NBC Ring Experiment (Fratantoni & Glickson, 2002; Garraffo et al., 2003; Garzoli et al., 2003; Goni & Johns, 2001, 2003; Johns et al., 2003). Those rings present typically a mean radius of 200 km, SSH anomaly of 30 cm, surface and subsurface azimuthal velocity of 1 m/s and 15–20 cm/s, respectively, and can reach over 1,000 m deep (Didden & Schott, 1993; Fratantoni et al., 1995; Fratantoni & Glickson, 2002; Fratantoni & Richardson, 2006; Garraffo et al., 2003; Goni & Johns, 2003; Jochumsen et al., 2010; Johns et al., 2003; Pauluhn & Chao, 1999). NBC rings travel with an average propagation speed of 8–15 km/day toward the Caribbean, for 3–4 months, until interacting with the Antilles, where they start to coalesce (Didden & Schott, 1993; Fratantoni et al., 1995; Fratantoni & Glickson, 2002; Fratantoni & Richardson, 2006; Garzoli et al., 2003; Johns et al., 1990; Richardson et al., 1994). It is estimated that on average 3–7 rings are detached from NBC per year (Fratantoni et al., 1995; Fratantoni & Glickson, 2002; Fratantoni & Richardson, 2006; Garzoli et al., 2003; Jochumsen et al., 2010; Johns et al., 1990; Mélice & Arnault, 2017), yet some works indicated a rate of 8–9 rings/year (Garraffo et al., 2003; Johns et al., 2003). Although a lot is known about NBC rings dynamics, only few works performed a long-term study (Jochumsen et al., 2010; Mélice & Arnault, 2017; Sharma et al., 2009). Moreover, it is crucial to establish and understand the change of ring parameters and how they evolve through seasons and years to evaluate, for example, if there is a seasonal or year-to-year variation that could indicate periods of higher intensity, energy, or SSH anomaly.

Several methodologies were used to efficiently identify eddies and determine their centers and parameters. Initially, methodologies were based either on the geometric velocity fields of geostrophic currents or in altimetry maps of sea surface. Posteriorly, the methods started to be based on dynamical parameters. McWilliams (1990) was one of the firsts to use relative vorticity for eddy identification. This method was improved over the use of wavelet analysis on the vorticity field (Doglioli et al., 2007). Other parameter widely used was the Okubo-Weiss (OW), which quantifies the importance of rotation in relation to strain through geostrophic current data (Chaigneau et al., 2008). On the other hand, other works utilized only the geometry of the geostrophic velocity field for eddy identification, assuming these structures as coherent vortex if characterized by closed contour current lines (Nencioli et al., 2010; Sadarjoen & Post, 2000). More recently, hybrid methodologies which consider both geometric and physical aspects (i.e., OW parameter) of eddies began to stand out (Halo et al., 2014; Yi et al. 2014). Mkhinini et al. (2014) introduced the local normalized angular momentum (LNAM), a new dynamical parameter for eddy detection, which represents the normalized value of the angular momentum in a restricted area. This value will reach its extremum in the center of a solid core rotation (LNAM = +1 for cyclonic eddies and LNAM = −1 for anticyclonic). Currently, hybrid algorithms have become even more effective with the possibility of identification of eddy interaction

through merging and splitting events (Le Vu et al., 2018; Li et al., 2014). Therefore, the improvement on the methodologies used for eddy identification and tracking allows the characterization of the main dynamical parameters of these structures, such as: maximum azimuthal velocity (V_{max}), speed-based radius (R_{max}), and Rossby number (Ro), apart from the events of eddy interaction.

The angular momentum eddy detection and tracking algorithm (AMEDA) (Le Vu et al., 2018), will be used in this study for the identification of NBC rings occurrence, trajectories, and physical parameters. The main goal of this work is to apply the AMEDA, using SSH and geostrophic currents field data, in order to investigate the intra- and inter-annual variability of NBC rings occurrence and parameters. Also, an event of rings merging will be detailed in terms of parameters change, and identified trajectories will be commented. The significance of studying eddy merging and splitting events relies on the fact that these events are able to change eddy characteristics. Indeed, ring interaction can alter significantly eddy size, energy, and SSH signal, and the main cause of their occurrence are current-eddy-topography interactions and current variation (Cui et al., 2019). Furthermore, the study goes through the previously results observed in published articles on NBC rings, for comparison with this AMEDA analysis. The study is organized as follows: in Section 2 the database and the study area are explored. The application of the data to AMEDA is described and the parameters measured are defined. In Section 3 we highlight the inter- and intra-annual variability of NBC rings, emphasizing how changes are observed in terms of their parameters. We also describe how vertical temperature and salinity profile change within eddies, and analyze the 4 observed merging events between two NBC rings with tracking identified by AMEDA. Finally, our results are compared with previous studies. Conclusion is presented in Section 4.

2. Data and Methods

2.1. Database and Study Area

The data set used in this study consists of 24 years (January/1993–December/2016) of absolute SSH (i.e., geopotential height) and the components of the geostrophic current fields taken from "Global Observed Ocean Physics Temperature Salinity Heights and Currents Reprocessing"—ARMOR 3D, with ¼° spatial resolution (e.g., Guinehut et al., 2012; Mulet et al., 2012; Buongiorno Nardelli et al., 2016). This database results from the combination of sea level anomaly (SLA), SST, and sea surface salinity (SSS) data and in situ T, S vertical profiles measurements, presenting a global 3D weekly temperature, salinity, geostrophic velocities fields (Verbrugge et al., 2017). ARMOR 3D is available at Copernicus Marine Environment Monitoring Service (CMEMS) web portal (http://marine.copernicus.eu/services-portfolio/accessto-products/, product id: MULTIOBS_GLO_PHY_REP_015_002) with the newest Version 4, updated in April 2018. The product used here was the Version 3 (product id: GLOBAL_REP_PHYS_001_021). The domain of this work is restricted to the region 15°N–5°S, 63°W–45°W, which includes NBC retroflection area (ring generation), Amazon and Orinoco Rivers mouths, and the Lesser Antilles (ring demise). Indeed, NBC rings seems also to interact with Amazon and Orinoco waters (Ffield, 2005; Rudzin et al., 2017). In addition, radiating Rossby waves from the east also reach this region, influencing ring dynamics (Fratantoni & Richardson, 2006; Jochum & Malanotte-Rizzoli, 2003). We used data from 50 m deep, in order to reduce the surface signal of equatorial Rossby waves and also as an attempt to identify subsurface rings with a negligible surface signal. Finally, sea surface height anomaly (SSHa) were calculated based on the 24 years data. Taking the anomalies can filter the seasonal signal, that dominates the tropical Atlantic Ocean (Arnault & Cheney, 1994), allowing a better analysis of intra-annual variability.

2.2. Detection Algorithm and Measured Parameters

The AMEDA (Le Vu et al., 2018) was used. It is a hybrid algorithm, based not only on dynamical parameters, but also on geometrical properties of the velocity field. In AMEDA, while the extremum LNAM (dynamical) indicates eddy centers, the closed streamlines (geometrical) indicates eddies boundaries, characterizing a structure as an eddy only if the grid point corresponds for both constraints (Le Vu et al., 2018). For eddy tracking, the algorithm uses the local nearest neighbor (LNN) method (Le Vu et al., 2018) and it also has the capacity to identify merging and splitting events. AMEDA has been used in a few works in the last years. Ioannou et al. (2017) applied this algorithm for the study of Ierapetra Eddies on the Mediterranean Sea, while Garreau et al. (2018) used the tool for tracking an anticyclonic eddy in the Algerian Basin.

The geostrophic velocities from ARMOR 3D were applied to AMEDA for ring identification, tracking, interaction with neighboring eddies, and for computation of their parameters. The first baroclinic Rossby radius of deformation (R_d) was calculated for each grid point, based on Chelton et al. (1998). This radius is defined as the length scale of geostrophic stretching, and at the equator R_d values are typically in scales of hundreds kilometers (Chelton et al., 1998; Nurser & Bacon, 2014). Although a ¼° data set grid was used, the combination with the calculated R_d values is expected to be enough for normal functioning of AMEDA, since it is a robust algorithm for different space–time resolutions, and with tuneable parameters (Le Vu et al., 2018). Only the NBC rings that were clearly detached from the NBC retroflection and that crossed 55°W were taken into account in this analysis. Moreover, we maintained the default AMEDA configuration of excluding the eddies between the 5°N and 5°S equatorial band, since the NBC retroflection and rings trajectory are still further north. For each week of a ring occurrence, several parameters were measured. These parameters constantly varied from week to week and from ring to ring. Therefore, the week of maximum SSHa was chosen to be the representative for the rings. The parameters analyzed were: lifetime (weeks), R_{max} (km), V_{max} (m/s), Ro, KE (cm^2/s^2), and SSHa (in cm). Ring lifetime corresponds to the number of weeks that the ring was identified by AMEDA. R_{max} (in kilometers) indicates the radius of the closed streamlines corresponding to the module of the maximum azimuthal velocity (V_{max}, in m/s). Ro is the dimensionless Rossby number defined as: $Ro = V_{max}/(f R_{max})$, where f is the Coriolis parameter at ring latitude. Ring kinetic energy (KE) is calculated from the geostrophic velocity field, is defined as $KE = (u^2 + v^2)/2$, and represents the mean KE for all the grid points within each ring. Finally, as previously cited, SSH anomalies were taken based on the 24 years data, providing the SSHa parameter.

3. Results and Discussion

3.1. Observed Variability of NBC Rings Shedding Rates

It is important to initially highlight that this is the first study to apply an eddy detection algorithm for 24 years period in the NBC region. Although other works have also analyzed decadal time-series in NBC rings generation (Jochumsen et al, 2010; Mélice & Arnault, 2017), they did not used an eddy identification tool based on dynamical and geometrical constraints, identifying the NBC rings only by statistical analysis of sea level anomalies (Mélice & Arnault, 2017), or based on velocity fields of the modeled data (Jochumsen et al., 2010). In the analyzed 24 years period, 121 NBC rings were observed to detach from the NBC retroflection and cross the 55°W longitude line. It provides an average shedding rate of five rings per year. The results for each year are presented in Figure 1a. Overall, previous studies estimate a rate from 2 to 9 rings per year, which varies according to the period covered and the method used by the study (e.g., Didden & Schott, 1993; Garzoli et al., 2003; Jochumsen et al., 2010; Johns et al., 1990, 2003; Mélice & Arnault, 2017; Sharma et al., 2009). The comparison with other works, allow us to say that AMEDA results are reasonable. In fact, the ring shedding rate here obtained varied from a maximum of eight rings/year in 2005 to a minimum of three rings/year in 2006 (Figure 1a). However, the present study underestimated the average shedding rate when comparing with few others which pointed for a 7–9 rings/year average (Johns et al., 2003; Jochumsen et al., 2010). This fact is thought to be mainly due to the presence of subsurface NBC rings, which present the maximum velocity signal at 200 m and no apparent surface signal (Garraffo et al., 2003). Because the present work used only 50 m depth velocity fields data, possibly some subsurface NBC rings were not identified by AMEDA. Furthermore, Goni and Johns (2001), using altimeter data, identified 34 anticyclonic eddies from October 1992 to December 1998. In this study, which started to count from 1993, 29 NBC rings were identified from 1993 to 1998. In addition, 18 NBC rings were observed using ocean color imagery from September 1997 to September 2000 (Fratantoni & Glickson, 2002), while we identified 16 NBC rings in the same period. Using in situ data from moorings and ship cruises, the NBC Rings Experiment (Garzoli et al., 2003; Goni & Johns, 2003; Johns et al., 2003) found one ring in November/December 1998, two rings from February/March 1999, and one ring in June/2000. In the present work, we identified the presence of all of these rings in the periods cited. The generation dates and parameters of all the 121 identified rings in this study are summarized in Supporting Information (Table S1). More recently, some works preceded in longer time series for NBC ring identification. Sharma et al. (2009) using drifting buoys, ADCP and satellite data identified 44 NBC rings in 8 years, with maximum shedding rates in 2005 and 2007, what is consistent with what was found in this study. Jochumsen et al. (2010) analyzed from the FLAME

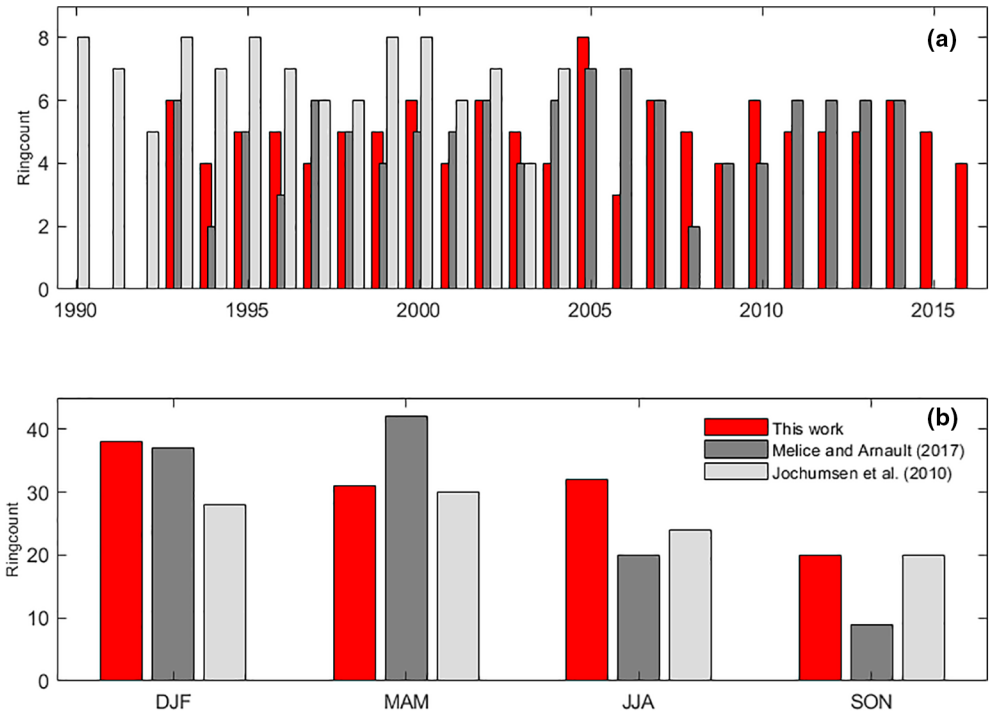

Figure 1. (a) Number of North Brazil Current (NBC) rings which crossed 55°W observed per year. (b) NBC rings seasonal climatology generated for 24 years period. Both (a) and (b) compare our results with Mélice and Arnault (2017) and Jochumsen et al. (2010).

model all the NBC ring types generation in 15 years, indicating a shedding rate ranging from 4 to 8 rings/year. In addition, the recent study from Mélice and Arnault (2017), using satellite altimeter and empirical mode decomposition, presented a mean rate of five rings generated by year, similar to the present study. Finally, although previous studies demonstrate some differences in the inter-annual ring generation rates, the similarities observed between them and the present work indicate AMEDA algorithm robustness and efficiency for ring surveillance, since it identified the presence of NBC rings quite similarly to other studies using different methods. It is thought that when applying current velocity data from greater depths rather than only surface fields, the algorithm will also be able to recognize rings of larger subsurface signal.

Moreover, it is possible to notice a considerable year-to-year variability in NBC ring generation. This rate remained between 4 and 6 rings/year, (Figure 1a), in exception from 2005 to 2006, where the maximum and minimum ring frequency, respectively, was observed. Sharma et al. (2009) theorized a biannual pattern in NBC ring generation rates, where alternate years present a gap in ring formation during late spring and early summer. Therefore, it seems that the maximum number of NBC rings generated in 2005 was compensated by the lower generation rate in the following year. The year 2005 has maximum shedding rates and appears to be followed by a steady cycle of ring formation and migration (Sharma et al., 2009). It is still not clear which mechanisms drive this inter-annual variability on NBC ring generation. However, few works have pointed possible reasons for it, such as: penetration latitude (i.e., distance between the northernmost point of the retroflection and the arbitrary location of 0°S, 42°W) of NBC retroflection (Garzoli et al., 2003) and the influence of large-scale transport processes in Atlantic Basin (Goni & Johns, 2003). Garzoli et al. (2003) indicated that almost every time NBC retroflection reaches its northernmost position, a ring is detached, although no clear seasonality is observed in NBC latitude of penetration. In addition, Goni and Johns (2003) speculated at least a weak relationship between ring generation and Northern Tropical Atlantic Index, based on possible links between ocean temperature variation and NBC rings shedding rate. Lastly, Sharma et al. (2009) indicated that ITCZ and forcing by trade winds are not the main factors influencing ring formation and migration. It is believed that several mechanisms might impact NBC rings generation, and further studies could highlight these relationships.

The results obtained for the ring generation as a function of the season are described in Figure 1b. We show that rings are formed in all months of the year, with a maximum ring generation in February, followed by March, June, and July. The minimum generation rate, in its turn, was observed in September-October-November trimester (SON) (Figure 1b). Those results agree with what was found in the literature, using different methods. Fratantoni et al. (1995) compared the modeled rings with observations from Richardson et al. (1994). They showed a maximum generation period from October to March, with the highest observation ring frequency in November and February, and the maximum modeled frequency in February, April, and May. Goni and Johns (2001) presented December and January as the months of greatest ring liberation. However, they have in 2003 pointed for different months as maximum (i.e., February and June) (Goni & Johns, 2003), which the latter agrees most with the current paper. Those previously cited works (Frantantoni et al., 1995; Goni & Johns, 2001, 2003) presented minimum generation rate from July to October, which is in agreement with the smaller generation in August and September observed in the present study. October 2016 was the only month in the analyzed period, which was characterized by more than one ring shed (Table S1).

The NBC ring maximum generation occurred from December to February (Figure 1b), while a minimum was observed from September to November. The December-January-February (DJF) trimester was responsible for 31.40% of NBC rings genesis in the 24 years, while 25.62% and 26.45% of rings were shed for March-April-May (MAM) and June-July-August (JJA) trimesters, respectively. It was verified a 47.37% reduction in ring generation rate between maxima (winter) and minima (fall) trimesters. Goni and Johns (2001) presented similar results using TOPEX altimetry data, with a maximum generation in boreal winter (DJF) and minimum in early boreal fall (SON), although from September to November the generation rate is quite the same as the previous months (MAM and JJA). On the other hand, Fratantoni and Glickson (2002) showed that the higher frequency of generation occurs from March to May, with equivalent frequency in the other trimesters. Also, Jochumsen et al. (2010) and Mélice and Arnault (2017) presented similar results on the number of rings generated per trimester, with the highest frequencies at spring (MAM) and minimum at fall (SON). According to Fratantoni and Glickson (2002), no particular seasonality is detected in NBC ring generation and that the observed variations in the results of those studies are most likely to be due to different methodologies. Seasonality appears to be evident but inconsistent between successive years (Sharma et al., 2009). Therefore, from the present and previous studies, it is possible to clearly identify the trimester of the minimum generation rates, which evolves the months of September, October, and November, and that NBC rings appear to be more frequent in the first half of the year.

3.2. NBC Rings Parameters

Figure S1 indicates the frequency distribution of the parameters for each identified ring. Those parameters were obtained at the time step corresponding to the week of maximum SSHa. The parameters of all the 121 identified rings in this study are summarized in Table S1. The NBC rings presented an average lifetime of 15.3 (±5.4) weeks, with the higher frequency of lifetimes between 10 and 18 weeks (Figure S1a). The last identified rings in October 2016 (i.e., R120 and R121) were not considered as they were not entirely vanished by the end of 2016, so their lifetime could not be determined. The maximum ring duration was 31 weeks, and the minimum, 4 weeks. These results are in agreement with previous studies (Goni & Johns, 2001; Richardson et al., 1994). Indeed, Goni and Johns (2003) verified through satellite altimetry that NBC rings remain an average of 3.5 months in the region, with this time ranging from 2 to 5 months. Besides, Fratantoni and Richardson (2006), using floats and drifters, pointed for a lifetime ranging from 1 to 6 months, with an average of 3.3 months. The importance of ring lifetime relies on how long the vortex dynamics is able to trap the parcel of water within it. The length scale of the ring, R_{max} ranged from a minimum of 87.3 km to a maximum of 204.8 km, with an average radius of 139.5 (±23.6) km. NBC rings were more frequent with R_{max} ranging from 120 to 160 km (Figure S1b). In general, other works on NBC rings indicate a similar length scale, with diameters varying from 150 to 400 km (Castelão & Johns, 2011; Didden & Schott, 1993; Fratantoni et al., 1995; Fratantoni & Glickson, 2002; Fratantoni & Richardson, 2006; Goni & Johns, 2003; Jochumsen et al., 2010; Richardson et al., 1994). These length scales of hundreds of kilometers imply a considerable water mass transport along the northern Brazilian coast. It is estimated that an annual transport of 9.3 Sv by NBC rings, which represents an essential part of the MOC return flow (Johns et al., 2003). A mean SSHa of 9.4 (±4.0) cm was detected with a maximum value of 24.0 cm. The higher frequency observed was

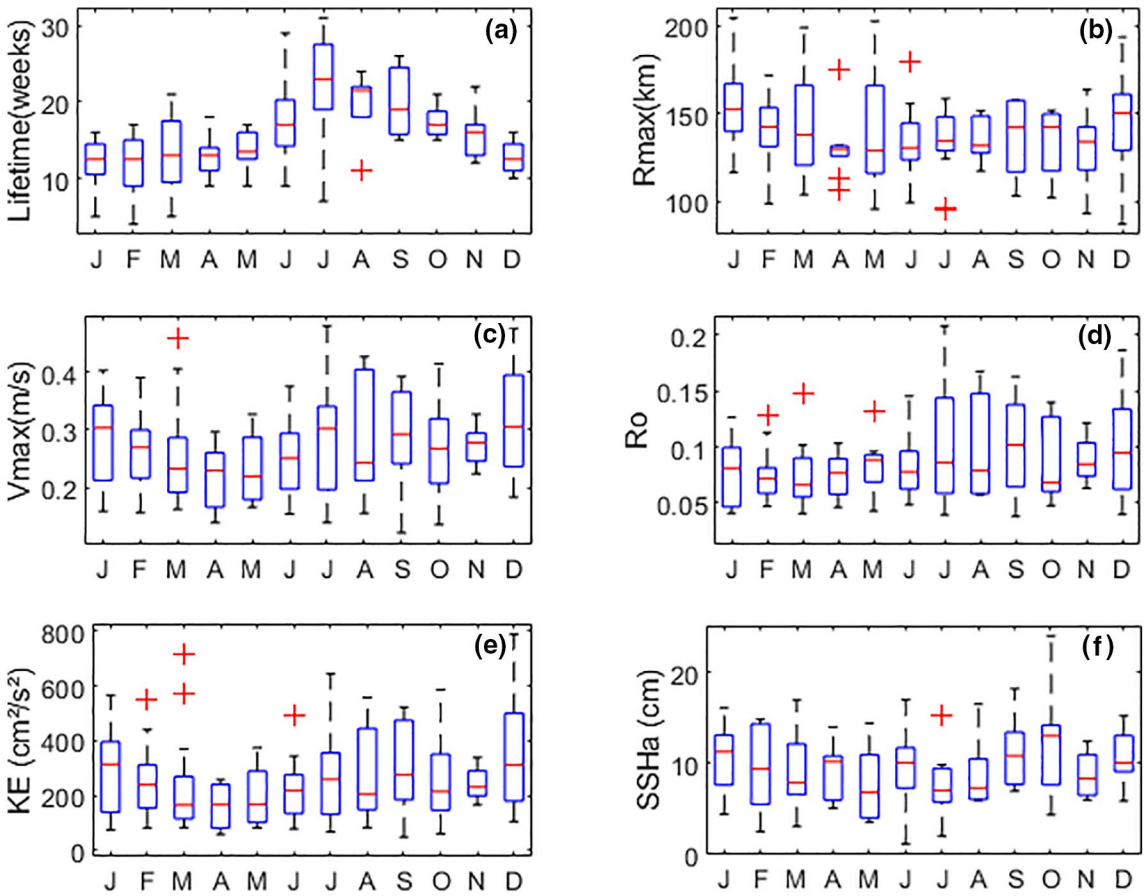

Figure 2. Monthly variation of the measured North Brazil Current rings parameter during the 24 years analysis: Ring lifetime (a), R_{max} (b), V_{max} (c), Rossby number (d), Kinetic Energy (e), SSH anomaly (f). The central red mark is the median, the edges of the box are the 25th and 75th percentiles, the whiskers extend to the most extreme datapoints, and individual red crosses are outliers.

around 5–15 cm of SSHa (Figure S1f). Those results are consistent with those found in the literature. Didden and Schott (1993) found a 4 cm SSH variability associated with NBC rings, while Goni and Johns (2001) presented an average SSH residue of 8 cm. More recently, maximum surface elevation related to NBC rings was pointed to range around 20–30 cm (Castelão & Johns, 2011; Cruz-Gómez & Salcedo-Castro, 2013). Moreover, the lowest observed value for SSHa was 1.1 cm, which might indicate that this study could also identify NBC rings with small surface signal, such as subsurface rings. However, to trustworthily classify NBC rings it is necessary to have a vertical picture of its dynamics, including thermocline and maximum velocity depths. Then, since the present work is based only on SSHa values and a 1-level velocity database, NBC ring classification goes beyond the scope of this study.

The frequency of the maximum azimuthal velocity values (V_{max}) computed from the NBC rings indicate a higher occurrence of rotational velocities from 20 to 30 cm/s (Figure 2c). The mean V_{max} is 0.27 (±0.08) m/s, while the maximum and minimum are 0.48 m/s and 0.12 m/s, respectively. Previous works indicate that NBC rings swirl velocity vary from 12 to 84 cm/s (Fratantoni et al., 1995; Fratantoni & Richardson, 2006; Richardson et al., 1994). However, more recent studies established that V_{max} could be even higher than 115 cm/s (Castelão & Johns, 2011; Cruz-Gómez & Salcedo-Castro, 2013). The reduced V_{max} found in this study might be explained by several reasons. First, the week of maximum SSHa does not necessarily correspond to the time step of maximum V_{max} . Then, it is possible that the values of V_{max} are not the maximum rotational velocities that a ring reached during its lifetime. In addition to this, when using geostrophic velocities fields and assuming geostrophic balance within an eddy, its azimuthal velocity might be underestimated due to the negligence of inertial components of momentum balance (Douglass & Richman, 2015). Hence, V_{max} values seemed to be underestimated in the present study. In addition to this, it is believed that

the cyclogeostrophic force terms are important in disrupting eddy characterization from geostrophy in eddies with Ro > 0.3 (Douglass & Richman, 2015). It seems from the literature that NBC rings Ros are on the threshold of these values, in a way that only geostrophy might not characterize NBC rings perfectly. Moreover, Iouannou et al. (2019) indicated the need of ageostrophic corrections for mesoscale anticyclones which exceeds Ro > 0.15. Hence, aiming to quantify the amplitude of the ageostrophic velocity component, we performed velocity corrections for NBC rings with Ro equals or exceeding 0.15, based on the methodology of Ioannou et al. (2017). Results for velocity profiles corrections and percentual increase in V_{max} for each of the eight analyzed rings are indicated in Figure S2 and Table S2, respectively. We verified a 30.0% average increase in cyclogeostrophic V_{max} for those rings. Plus, the Pearson correlation index between Ro and V_{max} increases for each ring ($p = 0.929$), showing the proportional increase in cyclogeostrophic V_{max} in relation to a larger Ro, as expected and indicated by Ioannou et al. (2019). Although in this study only a few rings exceed Ro > 0.15, it is clear that ageostrophic corrections for rings with large Ro are indeed not negligible for reliable V_{max} estimation.

Ro compares the importance of relative to planetary vorticity, and their values are variable around the globe. The high Ro values observed for the NBC rings region are due to the proximity of equator, an area of minimal Coriolis parameter. In this study, NBC rings presented an average Ro of 0.08 (±0.04) (Figure S1d), and maximum and minimum values of 0.21 and 0.04, respectively. Overall, it is expected that Ro values for anticyclones are negative. Yet, as we used the module of V_{max} to measure Ro, only positive values were found. AMEDA has already been used for Ro computation (de Marez et al., 2020; Garreau et al., 2018). The definition of Ro in the present work is the vortex Ro, which is based on maximal azimuthal velocity, and was also used by Fratantoni et al. (1995) and Castelão and Johns (2011). However, we highlight that various definitions of Ro exists and were applied for the NBC rings. Richardson et al (1994) and Cruz-Gómez and Salcedo-Castro (2013) defined Ro based on the core angular velocity (Ro(2) = Ω_0/f, $\Omega_0 = V(R)/R$ when R 0). For a Gaussian vortex, $V(r) = V_{max}/R_{max}\ r\ e$^((1 − r^2/[R_{max2}]/2), we get Ro(2) = 1.64*Ro. From the Ro definition, studies observed values between 0.13 and 0.26 (Fratantoni et al., 1995), and mean absolute Ro of 0.33 for the NBC region (Castelão & Johns, 2011). From Ro(2) values shifted from 0.20 to 0.36 (Richardson et al., 1994; Cruz-Gómez & Salcedo-Castro, 2013). Even though the 1.64 factor from Ro(2) to Ro, the values here obtained for Ro were still smaller than the ones cited in the literature using both definitions. As occurred for V_{max}, the use of purely geostrophic fields generated this underestimation. Douglass and Richman (2015) using the core vorticity Ro definition (Ro(3) = ζ0/f, for a Gaussian vortex Ro(3) = 3.3*Ro) indicated that ageostrophic corrections in V_{max} are needed for vortex Ro > 0.09. Here, we performed these corrections only for rings with Ro > 0.15, as previously cited (Figure S2 and Table S2), based on Ioannou et al. (2019). Table S2 also indicated the corrected cyclogeostrophic Ro for the eight analyzed rings.

Finally, the NBC rings KE in the present study varied from a minimum of 49.53 cm^2/s^2 to a maximum of 789.93 cm^2/s^2, with the highest frequency of rings with KE around 100–300 cm^2/s^2 (Figure S2e). The average kinetic energy observed was 255.30 (±154.81) cm^2/s^2. These results are in agreement with Didden and Schott (1993), who presented similar geostrophic NBC rings KE, changing from 100 to 300 cm^2/s^2. The increased standard deviation represents significant changes in rings KE, indicating that rings shed by the NBC present diverse dynamical characteristics from ring to ring.

In order to investigate the seasonal variation of NBC rings characteristics, the variability of their parameters is plotted as a function of the month for the 24 years (Figure 2). All months were characterized, at least in one year, by a NBC ring formation. NBC rings last less in boreal winter and have an increased lifetime in boreal summer, especially from July to August (Figure 2a). Although boreal summer months presented higher variability from minimum to maximum values, the median lifetime for these months is still higher than the others. On the other hand, R_{max} median values are increased in boreal winter (Figure 2b), even though a weak seasonal variability is observed. Sharma et al. (2009) also found low seasonal amplitude in NBC rings dimensions, with increased rings from October to March. Also, Ro and SSHa values did not present any clear seasonal variability (Figures 2d and 2f). In contrast, V_{max} and KE show the highest median values in boreal winter months (Figures 2c and 2e). V_{max} slightly increases in boreal summer, reaching a maximum in July. Similar behavior can be observed for KE. Didden and Schott (1993) associated KE changes in the NBC rings region with ring activity and the seasonal retroflection circulation, which, respectively, generated KE peaks in winter and a secondary summer maximum. More KE is available within NBC retroflection

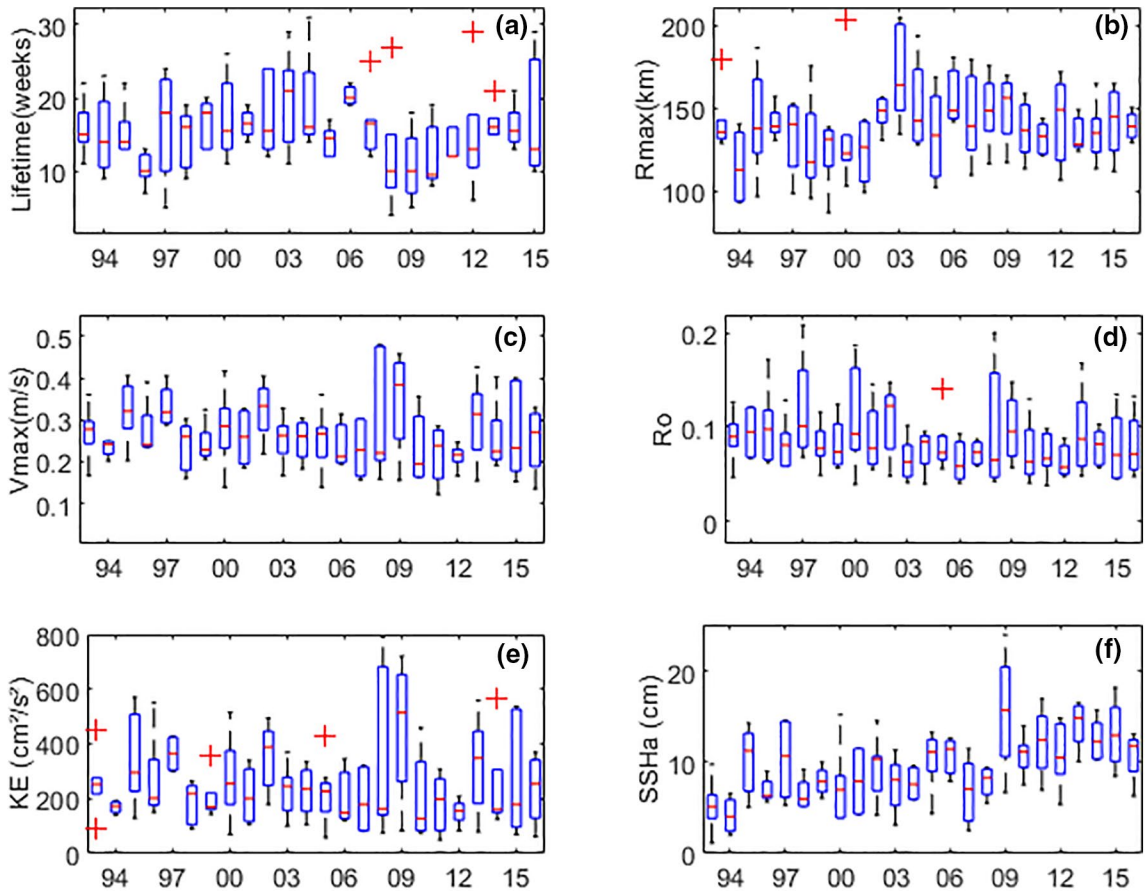

Figure 3. Year to year variability of the measured North Brazil Current rings parameters from 1994 to 2016. In exception, panel (a) only until 2015. Ring lifetime (a), R_{max} (b), V_{max} (c), Rossby number (d), Kinetic Energy (e), SSH anomaly (f). The central red mark is the median, the edges of the box are the 25th and 75th percentiles, the whiskers extend to the most extreme datapoints, and individual red crosses are outliers.

(Sharma et al., 2009). Therefore, V_{max} and KE follow NBC retroflection seasonality. The maximum strength of NBC retroflection in boreal summer (Richardson & Walsh, 1986) is verified in Figure 2c, while the maxima KE values are likely to be related to the beginning of NBC retroflection weakening in January (Lumpkin & Garzoli, 2005). The importance of studying such variability of parameters relies on the estimation of ring volume and energy within a ring, for example. Rings with larger dimensions are capable of wrapping a larger volume of water, while its lifetime indicates eddy capacity in maintaining that wrapped piece of water. At the same time, estimation on KE variation might indicate a seasonal energy transport within NBC rings. In general, NBC rings seem to have larger dimensions and rotate faster during boreal winter months, carrying more KE within them. This energy, however, is likely to dissipate more quickly, since, in boreal winter, NBC rings presented shorter lifetimes. On the other hand, NBC rings shed during summer, and early boreal fall appears to last longer, to have smaller diameters, and carry less energy.

The characteristics of the rings are plotted as a function of year to identify inter-annual variability (Figure 3). Ring lifetime is reduced in the last decade (Figure 3a). Very high values of lifetime are detected as outliers for some years (2007, 2008, 2012, and 2013). The highest ring dimension is in 2003, followed by 2006 and 2009 (Figure 3b). Sharma et al. (2009) pointed 2006 as the year with an average ring size larger than other years. The highest median rotational velocity was observed in 2009 (Figure 3c), following the year of maximum V_{max} variation (i.e., 2008). Year 2009 was also the year of maximum KE and mainly SSHa (Figures 3e and 3f). We calculated an annual climatological anomaly for the 24 years and observed that 2009 presented the most significant anomaly of V_{max}, KE, and SSHa (Figure 4). Foltz et al. (2012) identified an anomalous SST cooling in the Equatorial North Atlantic band (2°N–12°N) in 2009 and SST warming in the Equatorial South Atlantic (5°S–0°N) which produced a shift in wind direction, changed the ITCZ posi-

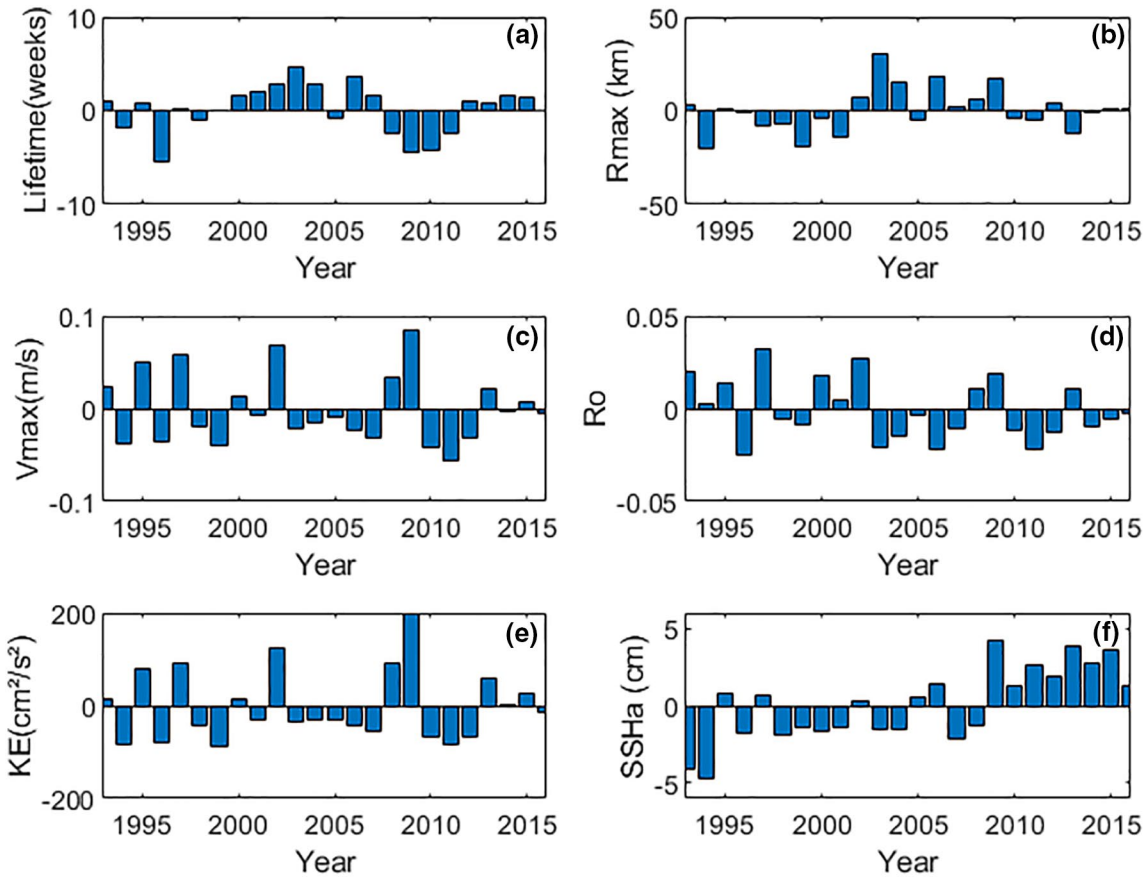

Figure 4. Averaged climatological anomaly of North Brazil Current ring parameters for each year during the 24 years analyzed: Ring lifetime (a), R_{max} (b), V_{max} (c), Rossby number (d), Kinetic Energy (e), SSH anomaly (f).

tion and the rainfall rates over the region. Moreover, Tyaquiçã et al. (2017) indicated an increased Amazon River discharge in 2009. These events might have altered current dynamics in this region, contributing to change NBC ring parameters in this year. We verified from filtered monthly anomalies of salinity and of zonal(u)-component of NBC in a longitudinal cut at 53°W, 3°N–7°N, from surface to 500 m deep, that 2009 year indeed presented an NBC intensity anomalous increase (Figure 5). This increase is indicated by a higher negative anomaly in the zonal component of NBC, and accompanied by salinity anomalies decease in the same year, showing a higher influence of Amazon plume in this year. Additionally, data for the 24 years of monthly Amazon discharge values recorded at the Óbidos Gauging Station, available from the Environmental Research Observatory– Geodynamical, hydrological, and biogeochemical control of erosion/alteration and material transport in the Amazon basin (ORE–HYBAM: http://www.ore-hybam.org), were used to estimate Amazon discharge inter-annual anomalies (Figure 5). From Amazon discharge is clear the positive anomaly during the entire 2009 year. An increased Amazon river runoff can contribute to NBC and its rings intensity by diminishing density through the influence of freshwater, generating an increase in current velocity. Moreover, Amazon river discharge could contribute to the increase in local vorticity, favoring rings intensity. Overall, it is believed that the combination of both increased NBC intensity and Amazon river runoff contributed for the 2009 intensity change in NBC rings dynamics. Another considerable pattern observed from 2009 is the positive trend in SSHa anomalies (Figure 4f). This indicates that SSHa within NBC rings is increasing in the last years. This could be related to changes in ocean circulation during the last decades. NBC rings are very dynamic and variable, being subject to several oceanographic and atmospheric forcings that affect their characteristics. Therefore, a strong inter-annual variability of their parameters is expected. In addition, we attempted to correlate Atlantic climate indexes with NBC parameter anomalies. The highest observed correlation was 0.34 between SSHa and Atlantic multidecadal oscillation (AMO). Although it seems a weak correlation, the analyzed period covered only the positive

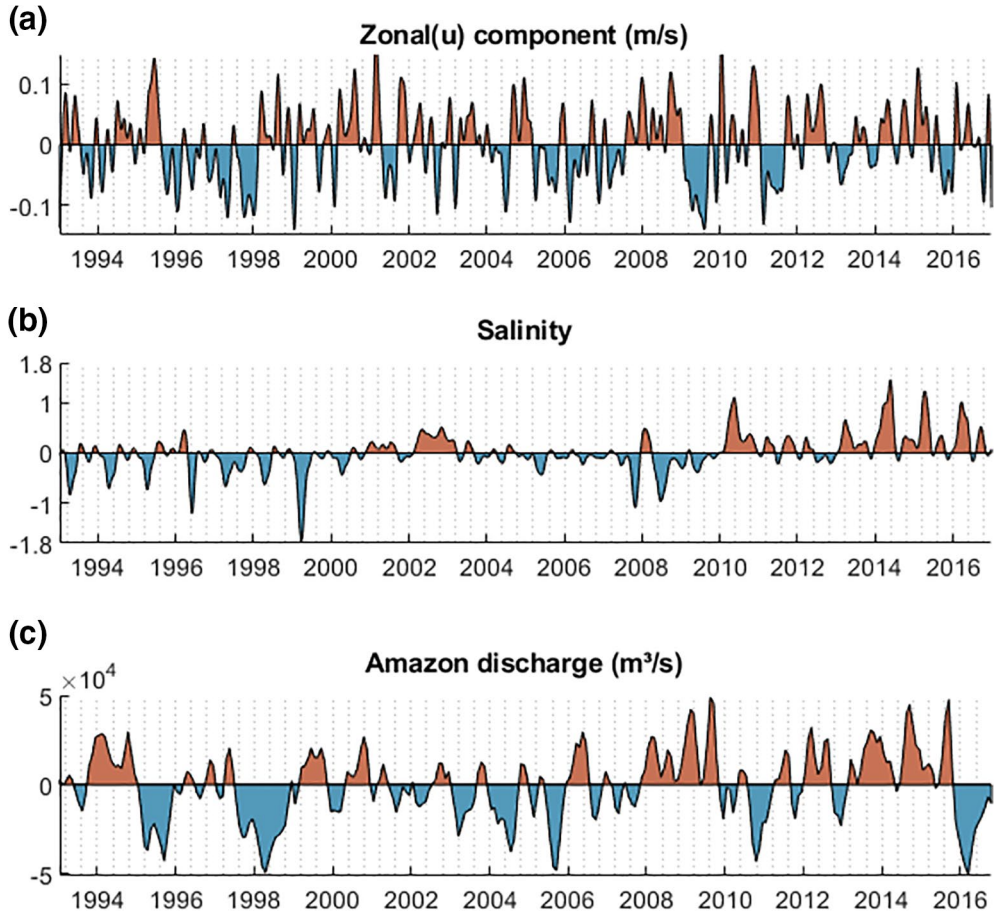

Figure 5. Monthly anomalies of zonal(u)-component (a) and salinity (b) of North Brazil Current in a longitudinal cut at 53°W, 3°N–7°N, from the surface to 500 m deep ARMOR 3D product. (c) Indicates monthly anomalies of Amazon river discharge at the Óbidos Gauging available from the ORE–HYBAM.

phase of the AMO cycle, characterized by changes in a climate signal of 60–80 years. Further studies could analyze a long-term climatological ring data to compare with this climate index. NBC ring evolution in terms of eddy characteristics is highlighted in Section 3.3.

3.3. Rings Trajectory and Evolution: Merged Rings Case Studies

Regarding the trajectory of the 121 analyzed NBC rings, Figure 6 and Table S3 displays the location of rings formation, location of maximum SSHa, and location of final detection. In general, we can observe rings being generated in the NBC retroflection area, propagating northwestward along the coast until demise when reaching the Lesser Antilles (Figure 6). The location of rings SSHa max is spread along the area, indicating that SSHa max could be observed right after ring formation as well as close to ring demise. Generation area is limited from 53°W to east, while ring final detection settles mainly from 58°W to west, although few rings were last identified east of this longitude. NBCRs far eastern from 58°W identified in Figure 6 indicate rings that merged (e.g., R83 – see Table S3). Rings centers demise were identified sitting northward or close to Barbados, and many were last verified before reaching Barbados. One ring translated differently, demising in the continental shelf near Orinoco River (Figure 6). Overall, rings decease occurred in regions influenced by the bottom bathymetry of Antilles. In fact, the influence of topography in finishing rings in the region has been well documented (Fratantoni & Richardson, 2006; Jochumsen et al., 2010). Additionally, their demise is strictly connected to the presence of the Lesser Antilles, which constitutes a barrier to ring translation (Fratantoni & Richardson, 2006). Interaction with the island leads to the destruction or the splitting of the incoming vortex into several smaller ones (Fratantoni & Richardson, 2006; Tanabe & Cenedese, 2008).

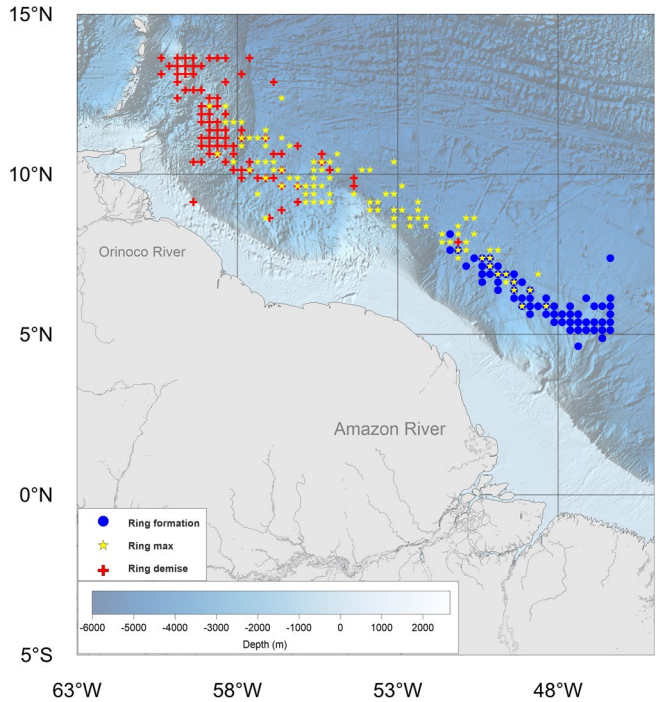

Figure 6. North Brazil Current rings position observed in the study area for three different moments during their lifetime: first week (blue); week of maximum sea surface height anomaly (yellow); last week (red). The background displays gridded bathymetry data from The General Bathymetric Charts of the Ocean (GEBCO), available at: https://www.gebco.net/.

Studies showed that ring might also be identified west of the island chain, indicating few surviving rings after topography interaction (Fratantoni & Richardson, 2006; Jochumsen et al., 2010; Mélice & Arnault, 2017; Tanabe & Cenedese, 2008). However, in our study the splitting of NBC rings encountering the Antilles was not detected by AMEDA, since the algorithm did not identify any NBCR west of the Antilles. This fact is mainly explained by the reduced study area, which imposes the tracking of rings with boundaries limited to 63°W.

Using rings center position (Table S3) and exploring the potential of ARMOR 3D data set for vertical profiles, we evaluated the water masses carried by NBC rings and the vertical temperature and salinity anomaly profiles on a seasonal scale. The vertical T-S diagrams were built from ARMOR 3D data set until 1,000 m, and the identified water masses were depicted (Figure 7). We recorded three water masses carried by NBC rings: South Atlantic Central Water (SACW), those with temperatures $\leq$ 18°C and salinities $\leq$ 36.0; coastal water (CW), with temperatures $\geq$ 20°C and salinities $\leq$ 35.4 and tropical water (TW), with temperatures $\geq$ 20°C and salinities $\geq$ 36.0. Neumann-Leitão et al. (2018) using in situ data observed the same water masses distribution in this region. Figure 7 displays the T-S diagrams for NBC rings locations at three different life stages, and starting at the four different seasons. A clear seasonality is observed in the water masses within NBC rings. From the end of boreal spring until JJA, CW from the Amazon river discharge is much more present in those eddies, while from September to February, the influence of TW is more pronounced is those vortex, and the CW is nearly absent (Figure 7). In fact, the seasonality of Amazon river runoff is known for decades, where the maximum monthly river discharge is in May and June (Hellweger & Gordon, 2002), demonstrating that the T-S diagram within an NBC eddy is related with their generation season. Additionally, NBC rings center presented similar T-S signatures during their translation, especially from their maxima week until their demise. It seems that rings in the starting week might not have enough intensity to trap water masses, reaching this stage of closed waters in vortex center during the following weeks. From the week of maxima SSHa, water masses are trapped until ring demise.

Furthermore, we performed the temperature and salinity 3-month profiles anomalies for each ring center identified, removing the climatology (based on the 24-years data from ARMOR 3D) from ring vertical profiles for each position. Three-month anomaly profiles were calculated in the central points of initial, maximum and final rings positions. The greatest anomalies observed in depth were located at ring SSHa maxima for both temperature and salinity (Figure 8). For initial and final positions, both the temperature and salinity anomalies profiles are not well defined, although rings initial position seems to relate to a stronger downward flux than final vortex locations (Figures S3a and S3b, respectively), since the latter is closer to Antilles bathymetry, what causes mixing. This behavior is an indication of an increased water downwelling in the eddy max position, while in initial and final positions the downward water flux at the ring center is weakened. Overall, regarding temperature profiles, maximum positive anomalies of 5°C are observed from 150 to 200 m deep, with no clear seasonality (Figure 8a). The downwelling associated with anticyclonic eddies increased the thermocline depth until 200 m in this region. Polo et al. (2015) indicated maxima MLD of 80 m for the WTNA region, showing that NBC rings can generate deeper thermocline and consequently greater mixed layer depths. For salinities, in general, negative anomalies (~-0.5) are observed at 100 m, settling above positive anomalies of 1.0 at 200 m (Figure 8b). These vertical salinity anomalies are also an indication of water sinking at NBC rings centers, that transport surface tropical saltier and coastal fresher waters to deeper layers. From this, the denser and saltier TWs settle under the less dense and fresher CW related to Amazon and Orinoco river plumes. Since Amazon discharge is more present in rings waters generated in JJA (Figure 7c), the most well-defined salinity anomalies profiles are referred to rings generated in this season, reaching SSHa max position at SON months, generating a more well-defined stratification in

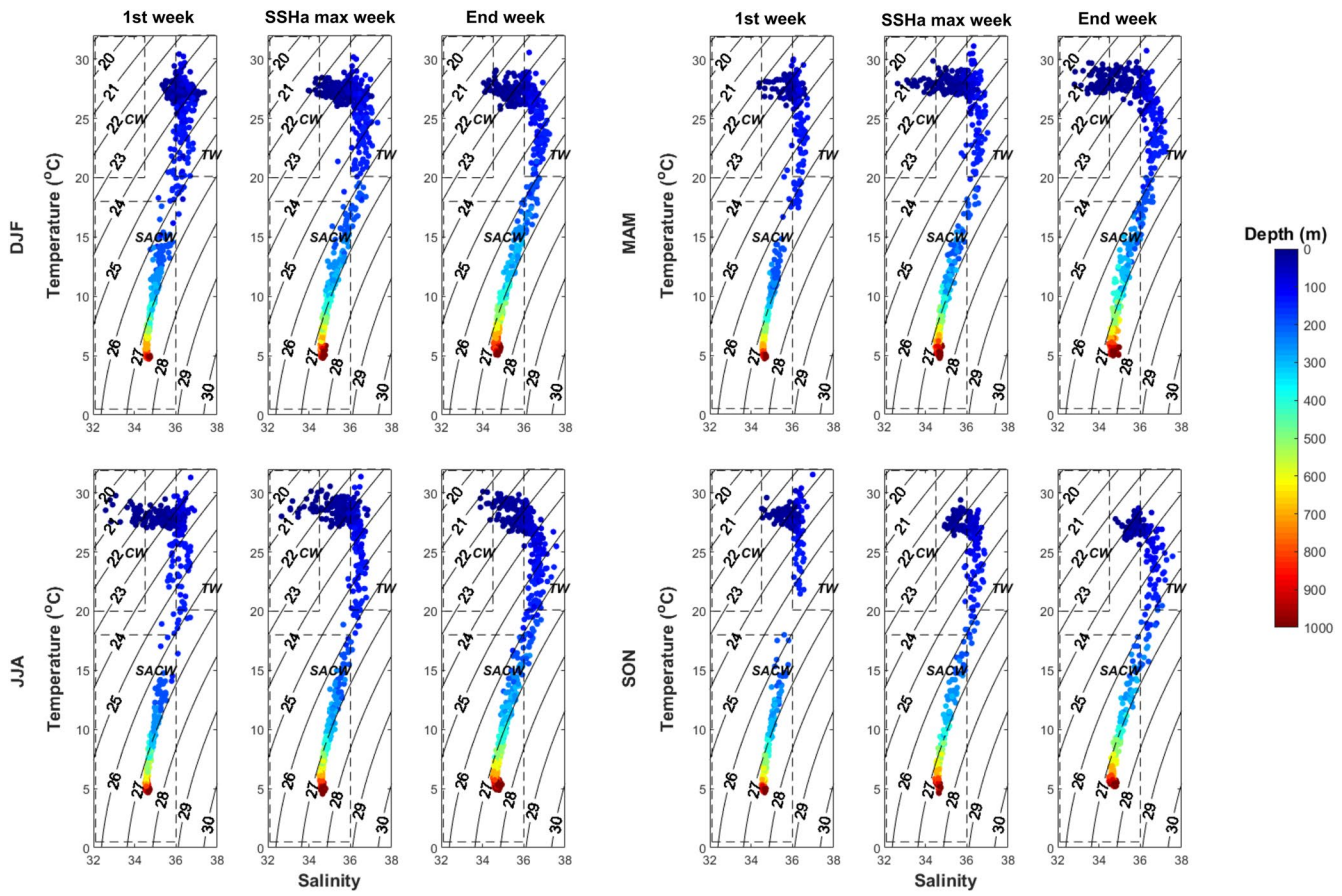

Figure 7. T-S diagram for each ring generated in the four different seasons from ARMOR 3D data set: DJF (a), MAM (b), JJA (c), SON (d). DJF, December-January-February trimester; JJA, June-July-August trimester; MAM, March-April-May trimester; SON, September-October-November trimester.

salinity anomalies profiles (Figure 8b). The increase in thermocline depth associated with sinking of riverine and TWs within NBC rings might spawn shifts on physical and biogeochemical features at WTNA, such as surface heat content, and CO_2 saturation. Further studies on this could indicate those answers.

A striking innovation of AMEDA algorithm is the capacity to detect merging between two eddies, and this capacity was explored in the present study. We detected only four merging rings events in the 24-year study period for NBC eddies, indicating that NBC rings did not interact much within each other. However, Castelão and Johns (2011) pointed that the presence of an inner core surrounded by an outer core of opposite vorticity is able to "isolate" the NBC rings, allowing them to be very close to each other without merging (Castelão & Johns, 2011). This structural configuration might explain why only 1 merging event was identified for each 6 years on average in the present study. In addition, few moments of NBC ring interaction with westward propagating anticyclonic eddies could be observed during the analyses. Plus, cyclonic eddies were also identified in certain weeks (Figure 9). Previous studies pointed for the formation of two different types of anticyclones in the region, the intermediate ones, and the NBC rings, that could coalesce within each other and generate deep-reaching rings (Garraffo et al., 2003; Jochum & Malanotte-Rizzoli, 2003). Cui et al. (2019) found that eddy merging is not likely to happen between eddies with similar intensities. Instead, the most common to happen is a strong eddy merging with a weaker one. Therefore, it is possible that NBC rings interact more often with weaker eddies (e.g., intermediate eddies, cleavaged eddies, eddies associated with NECC-NBC flow) present in the region than with other true NBC rings. Preceding works also identified cyclonic eddies in the region (Didden & Schott, 1993; Fratantoni & Richardson, 2006), which are associated with the NBC/NECC system variability, as well as with the dynamics of the anticyclonic NBC rings.

In order to highlight the typical evolution of the dynamical parameters of NBC rings during their northwestward propagation along the coast, and to analyze if there are significant changes in rings parameters

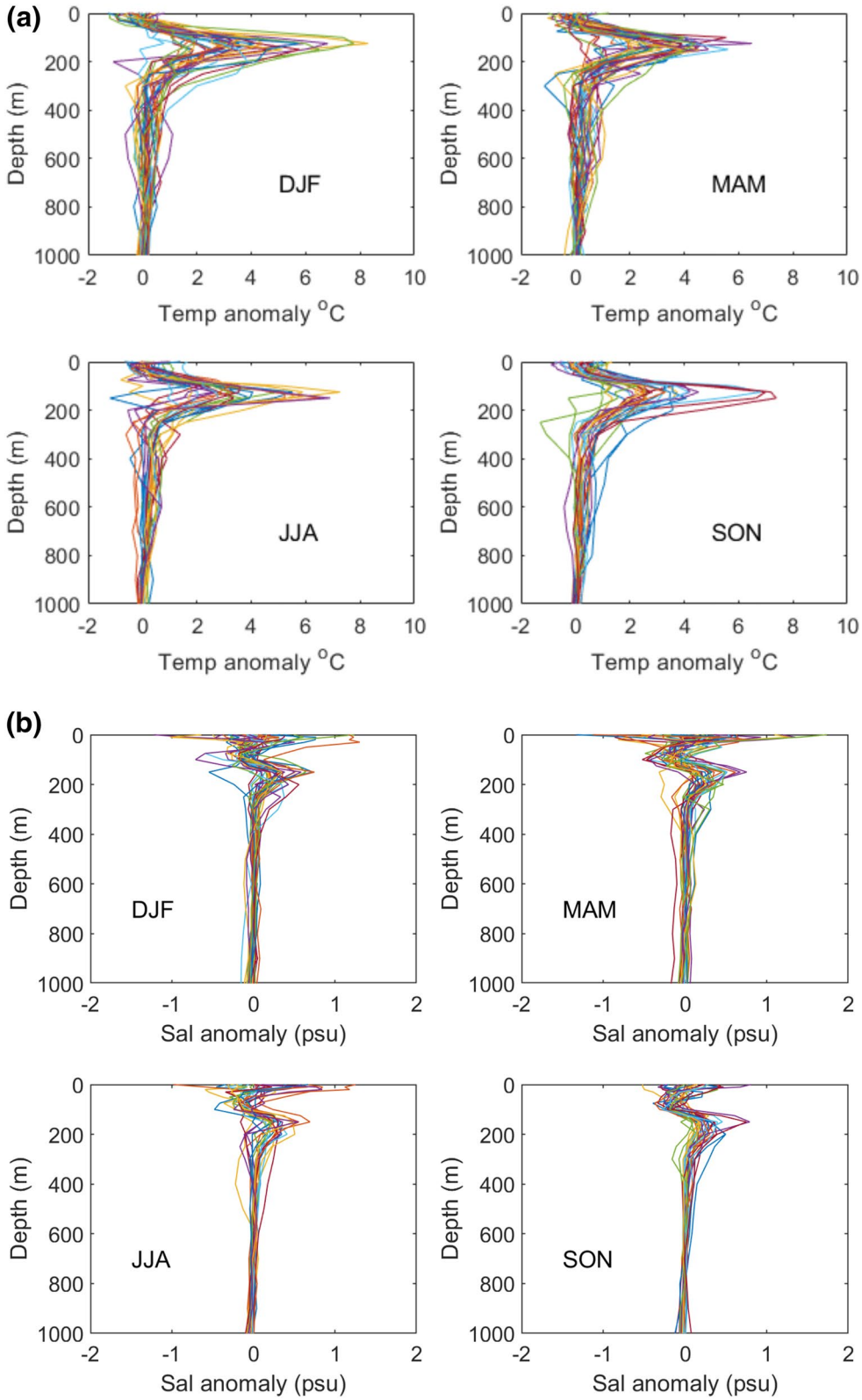

Figure 8. Temperature (a) and salinity (b) profiles anomalies for each ring center identified for Max sea surface height anomaly position, removing the climatology from ring vertical profiles for each position.

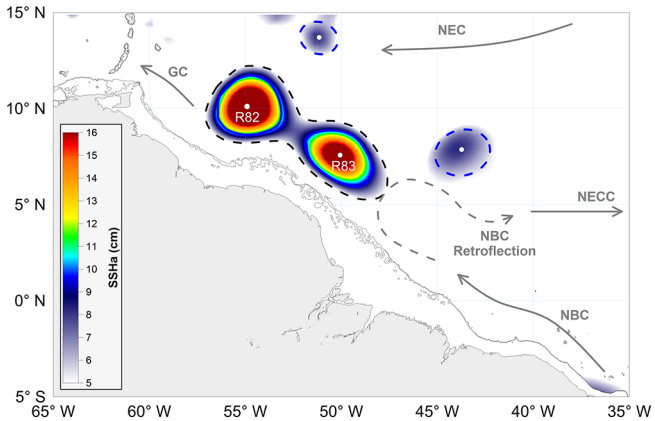

Figure 9. Large scale circulation features in Western Tropical North Atlantic over a sea surface height anomaly (SSHa) background from ARMOR 3D data set at week of 24th March 2009. R82 and R83 are two North Brazil Current (NBC) rings and two anticyclonic eddies identified by angular momentum eddy detection and tracking algorithm. Dashed (filled) lines represents outermost (R_{max}) closed contour R_{max}. Blue contours indicate anticyclonic eddies. Gray lines denotes large scale currents. SSHa smaller than 5 cm were removed for better visualization of rings. NECC, North Equatorial Countercurrent.

after merging, we computed the parameters for every week of occurrence of the 8 isolated rings which turned to four merged rings events. Rings parameters evolution is depicted in Figure S4 and Table S4. Weeks with NaN values represent weeks that AMEDA could not identify eddy. Figure 10 shows the trajectories of rings in the four analyzed events. From the four events, three rings remained merged until their demise (Figures 10a, 10c, 10d), while one of them merged and then splitted into two rings after 2 weeks (Figure 10b). All observed merging rings were generated from 52°W to east, above 5°N, and traveled northwestward along the northern coast of Brazil (Figure 10). Plus, the four merging events took place from mid-February to start of April, where six isolated rings were generated in DJF, one in September and one in March. Dated only in the first half of the year, the time of merging events corresponds with the time of increased ring formation (Figure 1). Other works also observed merging events only in this period (Barnier et al., 2001; Fratantoni & Richardson, 2006). It is believed that in the second half of the year the ring generation rate is not sufficient to promote a ring encounter when translating, before one of them demise in the Antilles. Still, regarding the location of merging events, all 4 events settled in the area indicated by the red rectangle in Figure 10. This area is located in a topographic depression between the start of Caribbean topography and the extended continental shelf from 53°W to 55°W (Figure 10). It is hypothesized that in this highlighted region NBC rings decelerate as reaching Antilles topography, allowing upcoming NBC rings to reach the previous eddy and merge. In fact, Barnier et al. (2001) indicated that a NBC eddy was slowed down as it encountered the Trinidad–Tobago topographic rise, which contributed for ring merging. The authors still indicated that such ring merging was also reported by Didden and Schott (1993). Further studies on the influence of this topography for the fusion of NBC rings are required. Lastly, Figure 10 also displays that rings trajectory right after merging are slightly deviated to west-southwest. De Marez et al. (2020) indicated that anticyclonic eddies are more likely to be orientated southwest-northeast due to the β-effect. It seems that NBC rings are also influenced by this effect.

In addition, the change on NBC ring vertical and translation structure is related not only to ring and current field dynamics but also to the influence of topography in the region, especially regarding ring demise (Fratantoni & Richardson, 2006; Jochumsen et al., 2010). Hence, since ring parameters evolve in time and could be strongly affected by bottom bathymetry, especially when the vortexes reach Caribbean coastal shelves, we attempted to evaluate the influence of topography in NBCRs parameters. To do that, we used the merged events M1 and M4 (Table S4) as case studies for comparison of their parameters before and after reaching 58°W (i.e., where influence of bottom topography seems to increase), computing their characteristics only 1 week after they merged to remove merging effects, and performing t student tests. M3 merged after 58°W, where merging effects could superimpose topographic effects, so we did not consider this event as a case study. On the other hand, M2 splits when reaches 58°W, what could indicate bathymetry influence. For M1, we observed significant decrease in R_{max} ($p = 0.002$), while total ratio and V_{max} did not change ($p = 0.9432$ and $p = 0.7154$, respectively). In the case of M4, no shifts were observed at all (R_{max}, $p = 0.1740$; total ratio, $p = 0.7800$; V_{max}, $p = 0.1383$). By potential vorticity conservation, it was expected that when reaching shallow waters eddies would flatten and increase their size, while diminish their velocities. However, only a significant reduction in R_{max} was observed. This uncertainty might be due to effects of the bathymetry in the algorithm identification using this data set spatial resolution (1/4°), where further studies using an increased data resolution could better indicate current vectors around the island chain, improving ring identification, and allowing a finer evaluation of the effects of Lesser Antilles bathymetry in NBC ring parameters

Moreover, significant changes were observed for three parameters of NBC rings after rings merging. To address that, we performed *t*-student tests for the parameters computed for each of the eight isolated and the four merged NBC rings, which results are indicated in Table 1. We removed the weeks immediately before

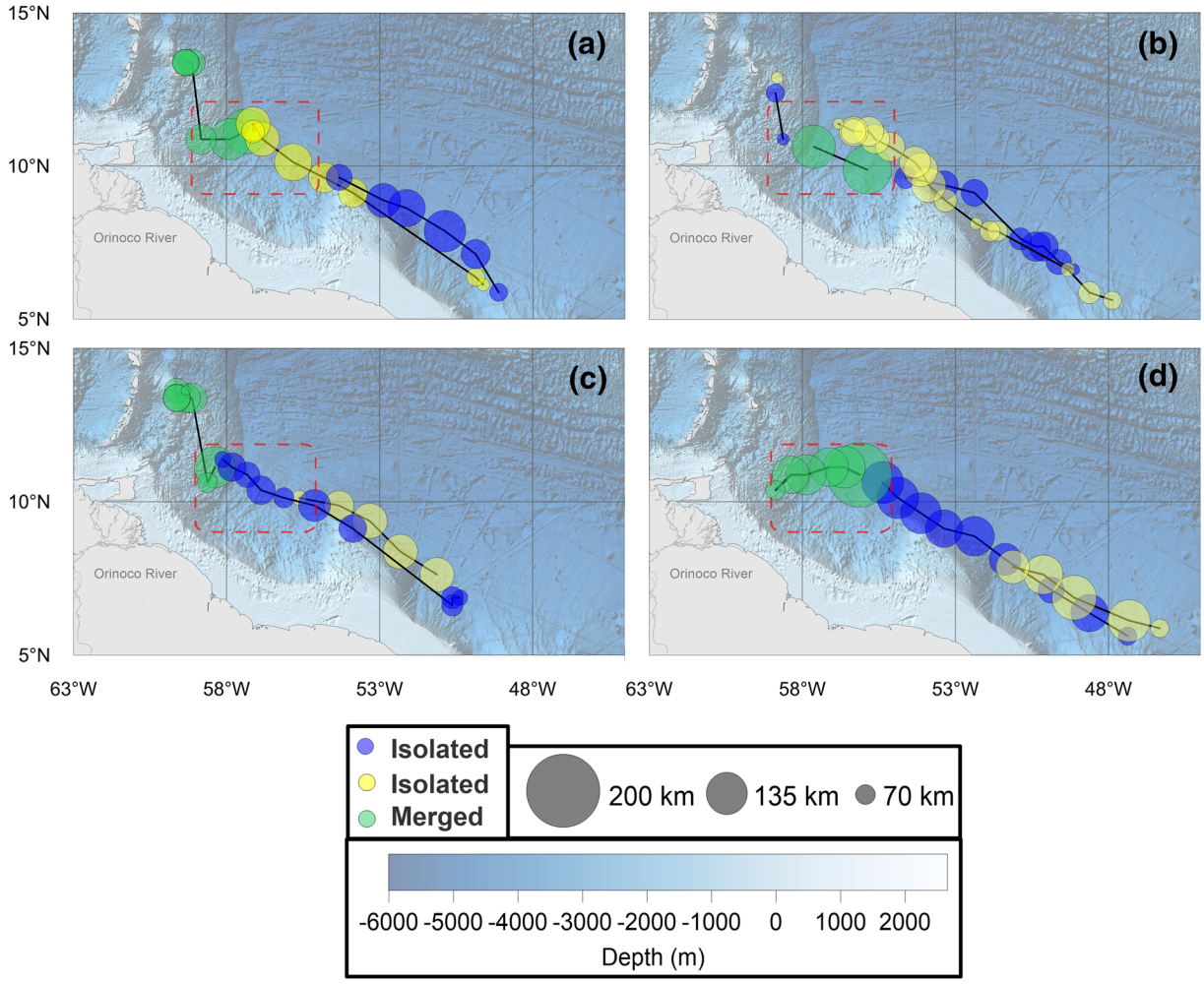

Figure 10. Merging rings trajectory. M1 from R20 (yellow) and R21 (blue) (a); M2 from R39 (yellow) and R40 (blue) (b); M3 from R78 (yellow) and R77 (blue) (c); M4 from R83 (yellow) and R82 (blue) (d). Red rectangle indicates area where all rings merged. Black lines represent rings trajectory. Circle size depicts R_{max}. Circle height is four times lower that the real circle height based on R_{max}. Circle shapes do not depict real ring shapes, are displayed only as ring representations.

Table 1
Test t-Student Between Isolated and Merged Rings

	t-student	Mean solo	Mean merged	Significant difference (%)
R_{max}	0.4091	113.6 km	121.2 km	NA
V_{max}	**0.0291**	0.23 m/s	0.28 m/s	**+22.0**
Ro	**0.0194**	0.11	0.08	**−27.3**
KE	**0.0141**	187.6 cm^2/s^2	285.1 cm^2/s^2	**+52.0**
SSHa	0.9775	6.4 cm	6.4 cm	NA

Note. Significant differences were considered in a 95% confidence interval ($p < 0.05$) and are indicated in bold. Significant difference (%) indicates the percentage of change between mean solo and mean merged rings parameters.

Abbreviations: KE, kinetic energy; Ro, Rossby number; SSHa, sea surface height anomaly.

and right after ring merging from the test t, in order to remove effects of definition of the eddy radius during the merging event, since for a perfect merging between two symmetric eddies their radii should tend to zero just before a single eddy contours emerge (Le Vu et al., 2018). Significant changes were verified for V_{max}, Ro and KE, while R_{max} and SSHa did not present considerable difference between isolated and merged vortex (Table 1). Shift in Ro occurred due to increased V_{max} and the maintenance of R_{max} from isolated to merged eddies. A V_{max} positive change of 22.0% resulted in merged rings with 52% more KE that the isolated, in average. This increase in ring KE might disrupt local circulation around Caribbean islands in a greater scale, impacting also fish larvae recruitment, and ocean-atmosphere energy exchanges. In addition, eddy merging events could function as a "large-scale energy pump" in the inverse energy cascades in two ways: from changes from small- to large-scale eddies and increasing residence time (Klein et al., 2019; Wang et al. 2019). After merging, there is a significantly increase the total KE and strengthen of the large geostrophic eddies by making them more coherent with a longer life time (Klein et al., 2019). In this study, however, we did not identified

shifts in R_{max} after merging (rings maintained their length scale), and due to interaction with Antilles right after merging did not allowed a longer residence time (i.e., they are not isolated eddies). Then, we cannot affirm that NBC rings play this role. Further studies on this might spark answers for this question. The increase ring KE was also observed by Cui et al. (2019). The authors reported that splitting or merging events can change eddy properties by a factor of 2 or more (Cui et al., 2019). The observed changes in this study did not represent such a variation in eddy properties after merging. However, it showed that NBC ring merging has a considerable impact in its rotational speed, KE and intensity variation, and that those events should be taken into account when evaluating physical and biogeochemical impacts of NBC rings in the WTNA. On the other hand, Wang et al. (2019) stated that, overall, eddies KE decreased while total mechanical energy increased after merging, and that merging events require external energy input into rings. Therefore, we theorized that only in specific years this necessary energy input coincided with times of NBC rings close enough to merge with each other, making a NBC ring merging event such a rare event. More studies on the relation of ring merging years and climate indexes that could provide the required amount of energy for rings merging might elucidate this hypothesis. To evaluate how ring parameters are related with each other, we performed a correlation analysis between the computed parameters for the eight isolated the four merged rings, where Pearson correlation index are indicated in Table S5. We observed that V_{max} and KE are well correlated with all analyzed parameters, in exception of Ro, while SSHa did not present high correlation with R_{max} . Therefore, the use of maximum KE as a proxy for rings maxima is more indicated than the SSHa used in this study, since it includes a correlation not only with ring speed and energy, but also with ring size.

4. Conclusions

We applied the AMEDA for the identification of NBC rings occurrence, trajectories, and physical parameters. This work uses a 24-year (1993–2016) reanalysis database of geopotential height and geostrophic velocity fields, standing as the first study to apply an eddy detection algorithm for NBC ring identification in a decadal period. The choice of AMEDA is based on its robustness and ease of use for eddy properties time series analysis, since it considers not only dynamical but also geometrical properties of the velocity field. Here, we identified an average rate of five NBC rings shed by year, which presented an average lifetime of 15.3 (±5.4) weeks, R_{max} from 87.3 to 204.8 km, with an average radius of 139.5 (±23.6) km, and were associated with mean SSHa within their centers of 9.4 (±4.0) cm. The mean observed V_{max} was 0.27 (±0.08) m/s, while the averaged Ro value was 0.08 (±0.04) and averaged KE was 255.3 (±154.8) cm^2/s^2. It is pointed that the azimuthal velocity and Ro values might be underestimated due to the use of purely geostrophic velocity fields.

NBC rings occur more frequently in the first half of the year. In fact, a decrease in ring generation rate of 47.37% was detected between maxima (boreal winter) and minima (boreal fall) trimesters. Moreover, NBC rings have larger dimensions, rotate faster, and present shorter lifetimes in boreal winter months, also carrying more KE within them. On the other hand, NBC rings shed last longer, have smaller diameters, and carry less energy during summer and early boreal fall. 2009 was a year of anomalous conditions, since it presented maximum values of KE, V_{max}, and SSHa associated with NBC rings. Another pattern identified in this work was the positive trend in SSHa anomalies from 2009 to 2016. This shows that SSHa within NBC rings is increasing in the last years, which could be further investigated.

Furthermore, we identified that downwelling within NBC rings center cause a thermocline deepening and anomalies in the salinity profile, indicating downward transport of tropical and CWs. Also, the analysis of T-S diagram allowed us to identify seasonality in relation to water masses in the interior of NBC rings. River water was observed within eddies center only in the ones formed from May to August, implying that NBC rings generated at those months might play different biogeochemical impacts in the WTNA region, such as shifts CO_2 fugacity in the ocean and CO_2 flux between ocean–atmosphere. The vertical change in temperature and salinity profiles can as well influence these physical and biogeochemical effects. More studies on this could provide this response. In addition, we observed in the year of 2009 a possible influence of Amazon river discharge on NBC ring dynamical parameters, such as V_{max} and KE, through effects in water density, flow vorticity and velocity, what might also have contributed for a ring merging event in that

year. Still, NBC rings merging events, although not very frequent, can significantly increase ring velocity and energy. However, the mechanism and energy supply that allow then to occur with NBC rings remains unclear. Moreover, these increase in ring KE can have an impact in the current dynamics around Caribbean, influencing, for example, phytoplankton distribution. Further works on this would provide this answer.

In this study, the use of reanalysis data associated with this AMEDA tool allowed the investigation of the intra- to inter-annual variability of NBC rings occurrence and dynamics. Further, the algorithm demonstrated to be straightforward in the identification of interaction among rings, which facilitate the analysis of these events. Overall, quantifying ring parameters seasonal and inter-annual variability, and identifying interaction between eddies, is crucial for understanding ring dynamics and consequently its impacts on the physics and biogeochemistry of the ocean.

Data Availability Statement

ARMOR 3D data supplied by Copernicus Marine Environment Monitoring Service (CMEMS) at http://marine.copernicus.eu/. The 24 years of monthly Amazon discharge values recorded at the Óbidos Gauging Station, are available from the Environmental Research Observatory– Geodynamical, hydrological, and biogeochemical control of erosion/alteration and material transport in the Amazon basin (ORE–HYBAM: http://www.ore-hybam.org).

Acknowledgments
This project was supported by the TRIATLAS project, which has received funding from the European Union's Horizon 2020 research and innovation program under grant agreement No 817578. The authors also acknowledge the support of the Brazilian Research Network on Global Climate Changes – Rede CLIMA (FINEP Grants 01.13.0353-00). The received funding did not lead to any conflict of interests regarding the publication of this manuscript. L. C. Aroucha thanks to Thomaz Arsouze, Briac Le Vu, and Alexandre Stegner for making AMEDA available and for the orientation of its use.

References

Arnault, S., & Cheney, R. E. (1994). Tropical Atlantic sea level variability from Geosat (1985–1989). *Journal of Geophysical Research*, *99*, 18207–18223. https://doi.org/10.1029/94JC01301

Barnier, B., Reynaud, T., Beckmann, A., Boning, C., Molines, J.-M., Barnard, S., & Jia, Y. (2001). On the seasonal variability and eddies in the North Brazil Current: insight from model intercomparison experiments. *Progress in Oceanography*, *44*, 195–230. https://doi.org/10.1016/S0079-6611(01)00005-2

Buongiorno Nardelli, B., Droghei, R., & Santoleri, R. (2016). Multi-dimensional interpolation of SMOS sea surface salinity with surface temperature and *in situ* salinity data. *Remote Sensing of Environment*, *180*, 392–402. https://doi.org/10.1016/j.rse.2015.12.052

Castelão, G. P., & Johns, W. E. (2011). Sea surface structure of North Brazil Current rings derived from shipboard and moored acoustic Doppler current profiler observations. *Journal of Geophysical Research*, *116*(C1). https://doi.org/10.1029/2010JC006575

Chaigneau, A., Gizolme, A., & Grados, C. (2008). Mesoscale eddies off Peru in altimeter records: Identification algorithms and eddy spatio-temporal patterns. *Progress in Oceanography*, *79*, 106–119. https://doi.org/10.1016/j.pocean.2008.10.013

Chelton, D. B., de Szoeke, R. A., Schlax, M. G., El Naggar, K., & Siwertz, N. (1998). Geographical variability of the first baroclinic Rossby radius of deformation. *Journal of Physical Oceanography*, *28*, 433–459. https://doi.org/10.1175/1520-0485(1998)028%3C0433:GVOTFB%3E2.0.CO;2

Cowen, R. K., Sponaugle, S., Paris, C. B., Lwiza, K., Fortuna, J., & Dorsey, S. (2003). Impact of North Brazil Current rings on local circulation and coral reef fish recruitment to Barbados, West Indies. In G. J. Goni & P. Malanotte-Rizzoli (Eds.), *Interhemispheric water exchange in the Atlantic Ocean, Elsevier Oceanographic Series* (Vol. 68, pp. 443–455), Amsterdam, Netherlands: Elsevier. https://doi.org/10.1016/S0422-9894(03)80157-5

Cruz-Gómez, R., & Salcedo-Castro, J. (2013). Analysis of horizontal and vertical ring structure based on analytical model and satellite data: Application to the North Brazil Current Rings. *Ocean Science Journal*, *48*(2), 161–172. https://doi.org/10.1007/s12601-013-0013-2

Cui, W., Wang, W., Zhang, J., & Yang, J. (2019). Multi core structures and the splitting and merging of eddies in global oceans from satellite altimeter data. *Ocean Science*, *15*, 413–430. https://doi.org/10.5194/os-15-413-2019

de Marez, C., Carton, X., L'Hégaret, P., Meunier, T., Stegner, A., Le Vu, B., & Morvan, M. (2020). Oceanic vortex mergers are not isolated but influenced by the β-effect and surrounding eddies. *Scientific Reports*, *10*(2897), https://doi.org/10.1038/s41598-020-59800-y

Didden, N., & Schott, F. (1993). Eddies in the North Brazil Current retroflection region observed by Geosat altimetry. *Journal of Geophysical Research*, *98*, 121–131. https://doi.org/10.1029/93JC01184

Doglioli, A. M., Blanke, B., Speich, S., & Lapeyre, G. (2007). Tracking coherent structures in a regional ocean model with wavelet analysis: Application to Cape Basin eddies. *Journal of Geophysical Research*, *112*(C5). https://doi.org/10.1029/2006JC003952

Douglass, E. M., & Richman, J. G. (2015). Analysis of ageostrophy in strong surface eddies in the Atlantic Ocean. *Journal of Geophysical Research: Oceans*, *120*, 1490–1507. https://doi.org/10.1002/2014JC010350

Ffield, A. (2005). North Brazil Current rings viewed by TRMM Microwave Imager SST and the influence on Amazon River Plume. *Deep Sea Research Part I Oceanographic Research Papers*, *52*, 137–160. https://doi.org/10.1016/j.dsr.2004.05.013

Foltz, G. R., McPhaden, M. J., & Lumpkin, R. (2012). A strong Atlantic Meridional Mode Event in 2009: The role of mixed layer dynamics. *Journal of Climate*, *25*, 363–380. https://doi.org/10.1175/JCLI-D-11-00150.1

Fonseca, C. A., Goni, G. J., Johns, W. E., & Campos, E. J. D. (2004). Investigation of the North Brazil Current retroflection and north equatorial countercurrent variability. *Geophysical Research Letters*, *31*. https://doi.org/10.1029/2004GL020054

Fratantoni, D. M., & Glickson, D. A. (2002). North Brazil Current ring generation and evolution observed with SeaWiFS. *Journal of Physical Oceanography*, *32*, 1058–1074. https://doi.org/10.1175/1520-0485(2002)032%3C1058:NBCRGA%3E2.0.CO;2

Fratantoni, D. M., Johns, W. E., & Townsend, T. L. (1995). Rings of the North Brazil Current: Their structure and behavior inferred from observations and a numerical simulation. *Journal of Geophysical Research*, *100*, 10633–10654. https://doi.org/10.1029/95JC00925

Fratantoni, D. M., Johns, W. E., Townsend, T. L., & Hurlburt, H. E. (2000). Low-latitude circulation and mass transport pathways in a model of the tropical Atlantic Ocean. *Journal of Physical Oceanography*, *30*, 1944–1966. https://doi.org/10.1175/1520-0485(2000)030%3C1944:LLCAMT%3E2.0.CO;2

Fratantoni, D. M., & Richardson, P. L. (2006). The evolution and demise of North Brazil Current Rings. *Journal of Physical Oceanography*, *36*, 1241–1264. https://doi.org/10.1016/S0422-9894(03)80154-X

Garraffo, Z., Johns, W. E., Chassignet, E., & Goni, G. (2003). North Brazil Current rings and transport of southern waters in a high resolution numerical simulation of the North Atlantic. In *Interhemispheric water exchange in the Atlantic Ocean, Elsevier Oceanography Series* (Vol. 68, pp. 375–410), Amsterdam: Elsevier. https://doi.org/10.1016/S0422-9894(03)80155-1

Garreau, P., Dumas, F., Louazel, S., Stegner, A., & Le Vu, B. (2018). High-resolution observations and tracking of a dual-core anticyclonic eddy in the Algerian Basin. *Journal of Geophysical Research: Oceans*, *123*(12), 9320–9339. https://doi.org/10.1029/2017JC013667

Garzoli, S. L., Ffield, A., & Yao, Q. (2003). North Brazil Current rings and the variability in the latitude of retroflection. In *Interhemispheric water exchange in the Atlantic Ocean, Elsevier Oceanography Series* (Vol. 68, pp. 357–373), Amsterdam: Elsevier. https://doi.org/10.1016/S0422-9894(03)80154-X

Goni, G. J., & Johns, W. E. (2001). A census of North Brazil Current rings observed from TOPEX/POSEIDON altimetry: 1992–1998. *Journal of Geophysical Research*, *28*, 1–4. https://doi.org/10.1029/2000GL011717

Goni, G. J., & Johns, W. E. (2003). Synoptic study of warm rings in the North Brazil Current retroflection region using satellite altimetry. In *Interhemispheric water exchange in the Atlantic Ocean, Elsevier Oceanography Series* (Vol. 68, pp. 335–356), Amsterdam: Elsevier. https://doi.org/10.1016/S0422-9894(03)80153-8

Guinehut, S., Dhomps, A.-L., Larnicol, G., & Le Traon, P.-Y. (2012). High resolution 3D temperature and salinity fields derived from in situ and satellite observations. *Ocean Science*, *8*, 845–857. https://doi.org/10.5194/os-8-845-2012

Halo, I., Backeberg, B., Penven, P., Ansorge, I., Reason, C., & Ullgren, J. (2014). Eddy properties in the Mozambique Channel: A comparison between observations and two numerical ocean circulation models. *Deep Sea Research Part II: Topical Studies in Oceanography*, *100*, 38–53. https://doi.org/10.1016/j.dsr2.2013.10.015

Hellweger, F. L., & Gordon, A. L. (2002). Tracing Amazon river water into the Caribbean sea. *Journal of Marine Research*, *60*, 537–549.

Ioannou, A., Stegner, A., Le Vu, B., Taupier-Letage, I., & Speich, S. (2017). Dynamical evolution of intense Ierapetra Eddies on a 22 year long period. *Journal of Geophysical Research: Oceans*, *122*(11), 9276–9298. https://doi.org/10.1002/2017JC013158

Ioannou, A., Stegner, A., Tuel, A., LeVu, B., Dumas, F., & Speich, S. (2019). Cyclostrophic corrections of AVISO/DUACS surface velocities and its application to mesoscale eddies in the Mediterranean Sea. *Journal of Geophysical Research: Oceans*, *124*(12), 8913–8932. https://doi.org/10.1029/2019JC015031

Jochum, M., & Malanotte-Rizzoli, P. (2003). On the generation and importance of North Brazil Current rings. *Journal of Marine Research*, *61*, 147–162. https://doi.org/10.1357/002224003322005050

Jochumsen, K., Rhein, M., Hüttl-Kabus, S., & Böning, C. W. (2010). On the propagation and decay of North Brazil Current rings. *Journal of Geophysical Research*, *115*(C10). https://doi.org/10.1029/2009JC006042

Johns, W. E., Lee, T. N., Beardsley, R. C., Candela, J., Limeburner, R., & Castro, B. (1998). Annual cycle and variability of the North Brazil Current. *Journal of Physical Oceanography*, *28*, 103–128. https://doi.org/10.1175/1520-0485(1998)028%3C0103:ACAVOT%3E2.0.CO;2

Johns, W. E., Lee, T. N., Schott, F. A., Zantopp, R. J., & Evans, R. H. (1990). The North Brazil Current retroflection: Seasonal structure and eddy variability. *Journal of Geophysical Research*, *95*, 22103–22120. https://doi.org/10.1029/JC095iC12p22103

Johns, W. E., Zantopp, R. J., & Goni, G. J. (2003). Cross-gyre transport by North Brazil Current rings. In G. J. Goni & P. Malanotte-Rizzoli (Eds.), *Interhemispheric water exchange in the Atlantic Ocean, Elsevier Oceanographic Series* (Vol. 68, pp. 411–441), Amsterdam: Elsevier. https://doi.org/10.1016/S0422-9894(03)80156-3

Klein, P., Lapeyre, G., Siegelman, L., Qiu, B., Fu, L., Torres, H., et al. (2019). Ocean-scale interactions from space. *Earth and Space Science*, *6*, 795–817. https://doi.org/10.1029/2018ea000492

Le Vu, B., Stegner, A., & Arsouze, T. (2018). Angular Momentum Eddy Detection and Tracking Algorithm (AMEDA) and its application to coastal eddy formation. *Journal of Atmospheric and Oceanic Technology*, *35*, 739–762. https://doi.org/10.1175/JTECH-D-17-0010.1

Legeckis, R., & Gordon, A. L. (1982). Satellite observations of the Brazil and Falkland currents – 1975 to 1976 and 1978. *Deep Sea Research Part A Oceanographic Research Papers*, *29*, 375–401. https://doi.org/10.1016/0198-0149(82)90101-7

Li, Q.-Y., Sun, L., Liu, S.-S., Xian, T., & Yan, Y.-F. (2014). A new mononuclear eddy identification method with simple splitting strategies. *Remote Sensing Letters*, *5*, 65–72. https://doi.org/10.1080/2150704X.2013.872814

Lumpkin, R., & Garzoli, S. L. (2005). Near-surface circulation in the tropical Atlantic Ocean. *Deep Sea Research Part I: Oceanographic Research Papers*, *52*, 495–518. https://doi.org/10.1016/j.dsr.2004.09.001

Ma, H. (1996). The dynamics of the North Brazil Current retroflection eddies. *Journal of Marine Research*, *54*, 35–53. https://doi.org/10.1357/0022240963213493

McWilliams, J. C. (1990). The vortices of two-dimensional turbulence. *Journal of Fluid Mechanics*, *219*, 361–385. https://doi.org/10.1017/S0022112090002981

Mélice, J.-L., & Arnault, S. (2017). Investigation of the intra-annual variability of the North Equatorial Countercurrent/North Brazil Current eddies and of the instability waves of the North tropical Atlantic Ocean using satellite altimetry and Empirical Mode Decomposition. *Journal of Atmospheric and Oceanic Technology*, *34*, 2295–2310. https://doi.org/10.1175/JTECH-D-17-0032.1

Mkhinini, N., Coimbra, A. L. S., Stegner, A., Arsouze, T., Taupier-Letage, I., & Beranger, K. (2014). Long-lived mesoscale eddies in the eastern Mediterranean sea: Analysis of 20 years of AVISO geostrophic velocities. *Journal of Geophysical Research: Oceans*, *119*, 8603–8626. https://doi.org/10.1002/2014JC010176

Mulet, S., RioMignot, M. -H. A., Guinehut, S., & Morrow, R. (2012). A new estimate of the global 3D geostrophic ocean circulation based on satellite data and in-situ measurements. *Deep Sea Research Part II: Tropical Studies in Oceanography*, *77–80*, 70–81. https://doi.org/10.1016/j.dsr2.2012.04.012

Nencioli, F., Dong, C., Dickey, T., Washburn, L., & McWilliams, J. (2010). A vector geometry-based eddy detection algorithm and its application to a high-resolution numerical model product and high-frequency radar surface velocities in the Southern California Bight. *Journal of Atmospheric and Oceanic Technology*, *27*(3), 564–579. https://doi.org/10.1175/2009JTECHO725.1

Neumann-Leitão, S., Melo, P. A. M. C., Schwamborn, R., Diaz, X., Figueiredo, L., Silva, A., et al. (2018). Zooplankton from a reef system under the influence of the Amazon River Plume. *Frontiers in Microbiology*, *9*, 355. https://doi.org/10.3389/fmicb.2018.00355

Nurser, A. J. G., & Bacon, S. (2014). The Rossby radius in the Arctic ocean. *Ocean Science*, *10*, 967–975. https://doi.org/10.5194/os-10-967-2014

Pauluhn, A., & Chao, Y. (1999). Tracking eddies in the subtropical North-Western Atlantic Ocean. *Physics and Chemistry of the Earth*, *24A*, 415–421. https://doi.org/10.1016/S1464-1895(99)00052-6

Polo, I., Lazar, A., Rodriguez-Fonseca, B., Mignot, J. (2015). Growth and decay of the equatorial Atlantic SST mode by means of closed heat budget in a coupled general circulation model. *Frontiers of Earth Science*, *3*, 37. https://doi.org/10.3389/feart.2015.00037

Richardson, P. L., Hufford, G. E., Limeburner, R., & Brown, W. S. (1994). North Brazil Current retroflection eddies. *Journal of Geophysical Research*, *99*, 5081–5093. https://doi.org/10.1029/93JC03486

Richardson, P., & Walsh, D. (1986). Mapping climatological seasonal variations of surface currents in the tropical Atlantic using ship drifts. *Journal of Geophysical Research*, *91*, 10537–10550. https://doi.org/10.1029/jc091ic09p10537

Rudzin, J. E., Shay, L. K., Jaimes, B., & Brewster, J. K. (2017). Upper ocean observations in eastern Caribbean Sea reveal barrier layer within a warm core eddy. *Journal of Geophysical Research: Oceans*, *122*, 1057–1071. https://doi.org/10.1002/2016JC012339

Sadarjoen, I. A., & Post, F. H. (2000). Detection, quantification, and tracking of vortices using streamline geometry. *Computers & Graphics*, *24*, 333–341. https://doi.org/10.1016/S0097-8493(00)00029-7

Sharma, N., Anderson, S. P., Brickley, P., Nobre, C., & Cadwallader, M. L. (2009). Quantifying the seasonal and inter-annual variability of the formation and migration pattern of *N*orth Brazil *C*urrent rings. Conference paper presented at OCEANS 2009, MTS/IEEE Biloxi – Marine Technology for Our Future: Global and Local Challenge, IEEE, pp. 1–7. https://doi.org/10.23919/OCEANS.2009.5422142

Tanabe, A., & Cenedese, C. (2008). Laboratory experiments on mesoscale vortices colliding with an island chain. *Journal of Geophysical Research*, *113*, C04022. https://doi.org/10.1029/2007JC004322

Tyaquiçã, P., Veleda, D., Lefèvre, N., Araujo, M., Noriega, C., Caniaux, G., et al. (2017). Amazon plume salinity response to ocean teleconnections. *Frontiers in Marine Science*, *4*, 250. https://doi.org/10.3389/fmars.2017.00250

Verbrugge, N., Mulet, S., Guinehut, S., & Buongiorno-Nardelli, B. (2017). ARMOR 3D: A 3D multi-observations T, S, U, V product of the ocean. *Geophysical Research Abstracts*, 19th EGU General Assembly, EGU2017, p. 17579.

Wang, Z.-F., Sun, L., Qiu-Yang, L., & Chemg, H. (2019). Two typical merging events of oceanic mesoscale anticyclonic eddies. *Ocean Science*, *15*, 1545–1559. https://doi.org/10.5194/os-15-1545-2019

Yi, J., Du, Y., He, Z., & Zhou, C. (2014). Enhancing the accuracy of automatic eddy detection and the capability of recognizing the multi-core structures from maps of sea level anomaly. *Ocean Science*, *10*, 39–47. https://doi.org/10.5194/os-10-39-2014

Zharkov, V., & Nof, D. (2010). Why does the North Brazil Current regularly shed rings but the Brazil Current does not? *Journal of Physical Oceanography*, *40*, 354–367. https://doi.org/10.1175/2009JPO4246.1